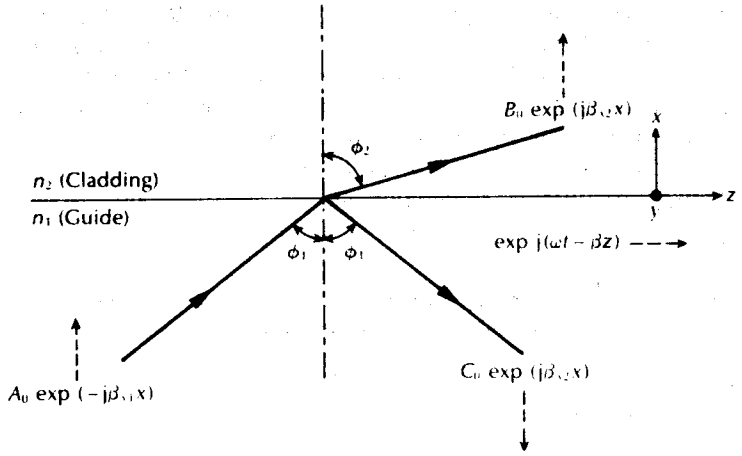

Figure 2.11 A wave incident on the guide–cladding interface of a planar dielectric waveguide. The wave vectors of the incident, transmitted and reflected waves are indicated (solid arrowed lines) together with their components in the z and x directions (dashed arrowed lines).

direction. Therefore from the discussion of Section 2.3.2 the wave propagation in the z direction may be described by $\exp j(\omega t - \beta z)$. In addition, there will also be propagation in the x direction. When the components are resolved in this plane:

$$\beta_{x1} = n_1 k \cos \phi_1 \tag{2.42}$$

$$\beta_{x2} = n_2 k \cos \phi_2 \tag{2.43}$$

where β_{x1} and β_{x2} are propagation constants in the x direction for the guide and cladding respectively. Thus the three waves in the waveguide indicated in Figure 2.11, the incident, the transmitted and the reflected, with amplitudes A, B and C, respectively, will have the forms:

$$A = A_0 \exp -(j\beta_{x1}x) \exp j(\omega t - \beta z) \tag{2.44}$$

$$B = B_0 \exp -(j\beta_{x2}x) \exp j(\omega t - \beta z) \tag{2.45}$$

$$C = C_0 \exp (j\beta_{x1}x) \exp j(\omega t - \beta z) \tag{2.46}$$

Using the simple trigonometrical relationship $\cos^2 \phi + \sin^2 \phi = 1$:

$$\beta_{x1}^2 = (n_1^2 k^2 - \beta^2) = -\xi_1^2 \tag{2.47}$$

and

$$\beta_{x2}^2 = (n_2^2 k^2 - \beta^2) = -\xi_2^2 \tag{2.48}$$

When an electromagnetic wave is incident upon an interface between two dielectric media, Maxwell's equations require that both the tangential components

of **E** and **H** and the normal components of **D** ($=\varepsilon\mathbf{E}$) and **B** ($=\mu\mathbf{H}$) are continuous across the boundary. If the boundary is defined at $x = 0$ we may consider the cases of the transverse electric (TE) and transverse magnetic (TM) modes.

Initially, let us consider the TE field at the boundary. When Eqs. (2.44) and (2.46) are used to represent the electric field components in the y direction E_y and the boundary conditions are applied, then the normal components of the **E** and **H** fields at the interface may be equated giving

$$A_0 + C_0 = B_0 \tag{2.49}$$

Furthermore it can be shown (see Appendix A) that an electric field component in the y direction is related to the tangential magnetic field component H_z following

$$H_z = \frac{\mathrm{j}}{\mu_r \mu_0 \omega} \frac{\partial E_y}{\partial x} \tag{2.50}$$

Applying the tangential boundary conditions and equating H_z by differentiating E_y gives:

$$-\beta_{x1} A_0 + \beta_{x2} C_0 = -\beta_{x2} B_0 \tag{2.51}$$

Algebraic manipulation of Eqs. (2.49) and (2.51) provides the following results:

$$C_0 = A_0 \left(\frac{\beta_{x1} - \beta_{x2}}{\beta_{x1} + \beta_{x2}} \right) = A_0 r_{ER} \tag{2.52}$$

$$B_0 = A_0 \left(\frac{2\beta_{x1}}{\beta_{x1} + \beta_{x2}} \right) = A_0 r_{ET} \tag{2.53}$$

where r_{ER} and r_{ET} are the reflection and transmission coefficients for the **E** field at the interface respectively. The expressions obtained in Eqs. (2.52) and (2.53) correspond to the Fresnel relationships [Ref. 11] for radiation polarized perpendicular to the interface (**E** polarization).

When both β_{x1} and β_{x2} are real it is clear that the reflected wave C is in phase with the incident wave A. This corresponds to partial reflection of the incident beam. However, as ϕ_1 is increased the component β_z (i.e. β) increases and, following Eqs. (2.47) and (2.48), the components β_{x1} and β_{x2} decrease. Continuation of this process results in β_{x2} passing through zero, a point which is signified by ϕ_1 reaching the critical angle for total internal reflection. If ϕ_1 is further increased the component β_{x2} becomes imaginary and we may write it in the form $-\mathrm{j}\xi_2$. During this process β_{x1} remains real because we have assumed that $n_1 > n_2$. Under the conditions of total internal reflection Eq. (2.52) may therefore be written as:

$$C_0 = A_0 \left(\frac{\beta_{x1} + \mathrm{j}\xi_2}{\beta_{x2} - \mathrm{j}\xi_2} \right) = A_0 \exp 2\mathrm{j}\delta_E \tag{2.54}$$

where we observe there is a phase shift of the reflected wave relative to the incident

wave. This is signified by δ_E which is given by:

$$\tan \delta_E = \frac{\xi_2^2}{\beta_{x1}} \tag{2.55}$$

Furthermore, the modulus of the reflected wave is identical to the modulus of the incident wave ($|C_0| = |A_0|$). The curves of the amplitude reflection coefficient $|r_{ER}|$ and phase shift on reflection, against angle of incidence ϕ_1, for TE waves incident on a glass–air interface are displayed in Figure 2.12 [Ref. 14]. These curves illustrate the above results, where under conditions of total internal reflection the reflected wave has an equal amplitude to the incident wave, but undergoes a phase shift corresponding to δ_E degrees.

A similar analysis may be applied to the TM modes at the interface, which leads to expressions for reflection and transmission of the form [Ref. 14]:

$$C_0 = A_0\left(\frac{\beta_{x1}n_2^2 - \beta_{x2}n_1^2}{\beta_{x1}n_2^2 + \beta_{x2}n_1^2}\right) = A_0 r_{HR} \tag{2.56}$$

and

$$B_0 = A_0\left(\frac{2\beta_{x1}n_2^2}{\beta_{x1}n_2^2 + \beta_{x2}n_1^2}\right) = A_0 r_{HT} \tag{2.57}$$

where r_{HR} and r_{HT} are, respectively, the reflection and transmission coefficients for the **H** field at the interface. Again, the expressions given in Eqs. (2.56) and (2.57) correspond to Fresnel relationships [Ref. 11], but in this case they apply to radiation polarized parallel to the interface (**H** polarization). Furthermore,

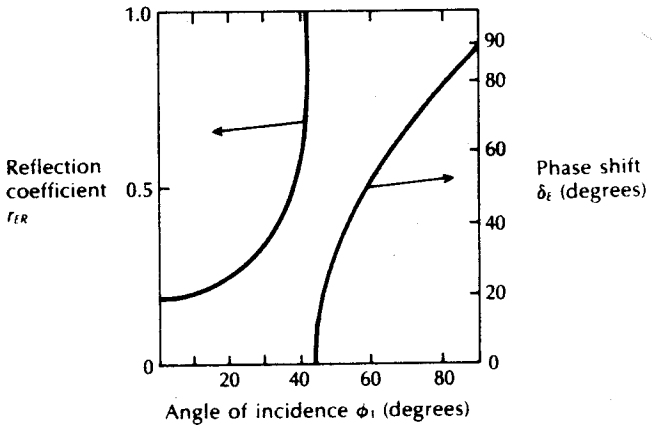

Figure 2.12 Curves showing the reflection coefficient and phase shift on reflection for transverse electric waves against the angle of incidence for a glass–air interface ($n_1 = 1.5$, $n_2 = 1.0$). Reproduced with permission from J. E. Midwinter, *Optical Fibers for Transmission*, John Wiley & Sons Inc., 1979.

considerations of an increasing angle of incidence ϕ_1, such that β_{x2} goes to zero and then becomes imaginary, again results in a phase shift when total internal reflection occurs. However, in this case a different phase shift is obtained corresponding to

$$C_0 = A_0 \exp(2j\delta_H) \tag{2.58}$$

where

$$\tan \delta_H = \left(\frac{n_1}{n_2}\right)^2 \tan \delta_E \tag{2.59}$$

Thus the phase shift obtained on total internal reflection is dependent upon both the angle of incidence and the polarization (either TE or TM) of the radiation.

The second phenomenon of interest under conditions of total internal reflection is the form of the electric field in the cladding of the guide. Before the critical angle for total internal reflection is reached, and hence when there is only partial reflection, the field in the cladding is of the form given by Eq. (2.45). However, as indicated previously, when total internal reflection occurs, β_{x2} becomes imaginary and may be written as $-j\xi_2$. Substituting for β_{x2} in Eq. (2.45) gives the transmitted wave in the cladding as:

$$B = B_0 \exp(-\xi_2 x) \exp j(\omega t - \beta z) \tag{2.60}$$

Thus the amplitude of the field in the cladding is observed to decay exponentially* in the x direction. Such a field, exhibiting an exponentially decaying amplitude, is often referred to as an evanescent field. Figure 2.13 shows a diagrammatic representation of the evanescent field. A field of this type stores energy and transports it in the direction of propagation (z) but does not transport energy in the

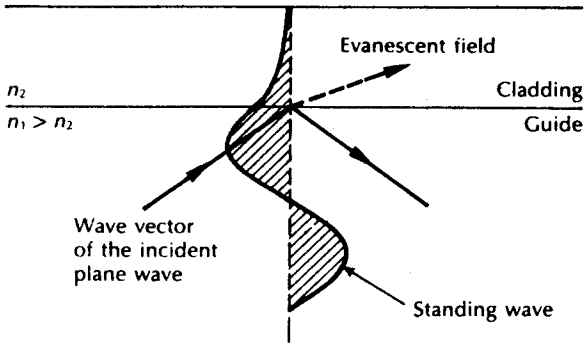

Figure 2.13 The exponentially decaying evanescent field in the cladding of the optical waveguide.

* It should be noted that we have chosen the sign of ξ_2 so that the exponential field decays rather than grows with distance into the cladding. In this case a growing exponential field is a physically improbable solution.

transverse direction (x). Nevertheless, the existence of an evanescent field beyond the plane of reflection in the lower index medium indicates that optical energy is transmitted into the cladding.

The penetration of energy into the cladding underlines the importance of the choice of cladding material. It gives rise to the following requirements:

1. The cladding should be transparent to light at the wavelengths over which the guide is to operate.
2. Ideally, the cladding should consist of a solid material in order to avoid both damage to the guide and the accumulation of foreign matter on the guide walls. These effects degrade the reflection process by interaction with the evanescent field. This in part explains the poor performance (high losses) of early optical waveguides with air cladding.
3. The cladding thickness must be sufficient to allow the evanescent field to decay to a low value or losses from the penetrating energy may be encountered. In many cases, however, the magnitude of the field falls off rapidly with distance from the guide–cladding interface. This may occur within distances equivalent to a few wavelengths of the transmitted light.

Therefore, the most widely used optical fibers consist of a core and cladding, both made of glass. The cladding refractive index is thus higher than would be the case with liquid or gaseous cladding giving a lower numerical aperture for the fiber, but it provides a far more practical solution.

2.3.5 Goos–Haenchen shift

The phase change incurred with the total internal reflection of a light beam on a planar dielectric interface may be understood from physical observation. Careful examination shows that the reflected beam is shifted laterally from the trajectory predicted by simple ray theory analysis, as illustrated in Figure 2.14. This lateral displacement is known as the Goos–Haenchen shift, after its first observers.

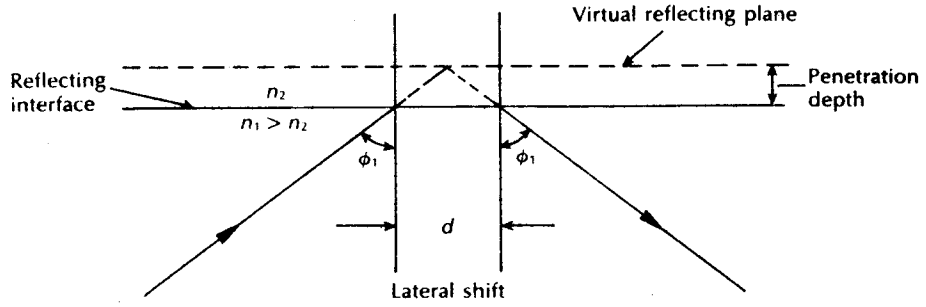

Figure 2.14 The lateral displacement of a light beam on reflection at a dielectric interface (Goos–Haenchen shift).

The geometric reflection appears to take place at a virtual reflecting plane which is parallel to the dielectric interface in the lower index medium, as indicated in Figure 2.14. Utilizing wave theory it is possible to determine this lateral shift [Ref. 14] although it is very small ($d \simeq 0.06$ to $0.10\ \mu$m for a silvered glass interface at a wavelength of $0.55\ \mu$m) and difficult to observe. However, this concept provides an important insight into the guidance mechanism of dielectric optical waveguides.

2.4 Cylindrical fiber

2.4.1 Modes

The exact solution of Maxwell's equations for a cylindrical homogeneous core dielectric waveguide* involves much algebra and yields a complex result [Ref. 15]. Although the presentation of this mathematics is beyond the scope of this text, it is useful to consider the resulting modal fields. In common with the planar guide (Section 2.3.2), TE (where $E_z = 0$) and TM (where $H_z = 0$) modes are obtained within the dielectric cylinder. The cylindrical waveguide, however, is bounded in two dimensions rather than one. Thus two integers, l and m, are necessary in order to specify the modes, in contrast to the single integer (m) required for the planar guide. For the cylindrical waveguide we therefore refer to TE_{lm} and TM_{lm} modes. These modes correspond to meridional rays (see Section 2.2.1) travelling within the fiber. However, hybrid modes where E_z and H_z are nonzero also occur within the cylindrical waveguide. These modes which result from skew ray propagation (see Section 2.2.4) within the fiber are designated HE_{lm} and EH_{lm} depending upon whether the components of **H** or **E** make the larger contribution to the transverse (to the fiber axis) field. Thus an exact description of the modal fields in a step index fiber proves somewhat complicated.

Fortunately, the analysis may be simplified when considering optical fibers for communication purposes. These fibers satisfy the weakly guiding approximation [Ref. 16] where the relative index difference $\Delta \ll 1$. This corresponds to small grazing angles θ in Eq. (2.34). In fact Δ is usually less than 0.03 (3%) for optical communications fibers. For weakly guiding structures with dominant forward propagation, mode theory gives dominant transverse field components. Hence approximate solutions for the full set of HE, EH, TE and TM modes may be given by two linearly polarized components [Ref. 16]. These linearly polarized (LP) modes are not exact modes of the fiber except for the fundamental (lowest order) mode. However, as Δ in weakly guiding fibers is very small, then HE–EH mode pairs occur which have almost identical propagation constants. Such modes are said to be degenerate. The superpositions of these degenerating modes characterized by a common propagation constant correspond to particular LP modes regardless of

* This type of optical waveguide with a constant refractive index core is known as a step index fiber (see Section 2.4.3).

their HE, EH, TE or TM field configurations. This linear combination of degenerate modes obtained from the exact solution produces a useful simplification in the analysis of weakly guiding fibers.

The relationship between the traditional HE, EH, TE and TM mode designations and the LP_{lm} mode designations are shown in Table 2.1. The mode subscripts l and m are related to the electric field intensity profile for a particular LP mode (see Figure 2.15(d)). There are in general $2l$ field maxima around the circumference of the fiber core and m field maxima along a radius vector. Furthermore, it may be observed from Table 2.1 that the notation for labelling the HE and EH modes has changed from that specified for the exact solution in the cylindrical waveguide mentioned previously. The subscript l in the LP notation now corresponds to HE and EH modes with labels $l+1$ and $l-1$ respectively.

The electric field intensity profiles for the lowest three LP modes, together with the electric field distribution of their constituent exact modes, are shown in Figure 2.15. It may be observed from the field configurations of the exact modes that the field strength in the transverse direction (E_x or E_y) is identical for the modes which belong to the same LP mode. Hence the origin of the term 'linearly polarized'.

Using Eq. (2.31) for the cylindrical homogeneous core waveguide under the weak guidance conditions outlined above, the scalar wave equation can be written in the form [Ref. 17]:

$$\frac{d^2\psi}{dr^2} + \frac{1}{r}\frac{d\psi}{dr} + \frac{1}{r^2}\frac{d^2\psi}{d\phi^2} + (n_1^2k^2 - \beta^2)\psi = 0 \tag{2.61}$$

where ψ is the field (**E** or **H**), n_1 is the refractive index of the fiber core, k is the propagation constant for light in a vacuum, and r and ϕ are cylindrical coordinates. The propagation constants of the guided modes β lie in the range:

$$n_2k < \beta < n_1k \tag{2.62}$$

Table 2.1 Correspondence between the lower order in linearly polarized modes and the traditional exact modes from which they are formed

Linearly polarized	Exact
LP_{01}	HE_{11}
LP_{11}	$HE_{21}, TE_{01}, TM_{01}$
LP_{21}	HE_{31}, EH_{11}
LP_{02}	HE_{12}
LP_{31}	HE_{41}, EH_{21}
LP_{12}	$HE_{22}, TE_{02}, TM_{02}$
LP_{lm}	$HE_{2m}, TE_{0m}, TM_{0m}$
LP_{lm} ($l \neq 0$ or 1)	$HE_{l+1,m}, EH_{l-1,m}$

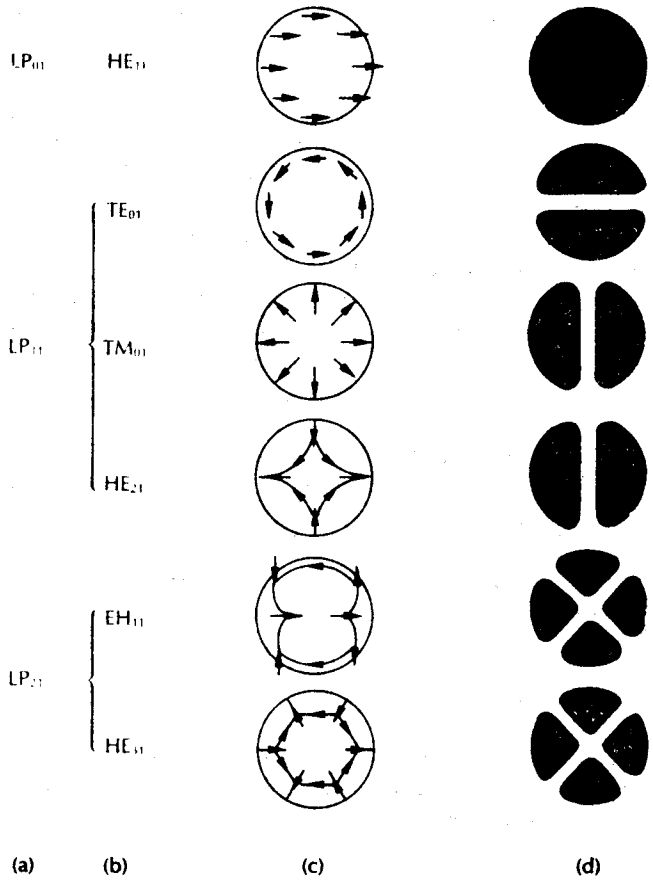

Figure 2.15 The electric field configurations for the three lowest LP modes illustrated in terms of their constituent exact modes: (a) LP mode designations; (b) exact mode designations; (c) electric field distribution of the exact modes; (d) intensity distribution of E_x for the exact modes indicating the electric field intensity profile for the corresponding LP modes.

where n_2 is the refractive index of the fiber cladding. Solutions of the wave equation for the cylindrical fiber are separable, having the form:

$$\psi = E(r)\left\{\begin{matrix}\cos l\phi \\ \sin l\phi\end{matrix}\right\} \exp\,(\omega t - \beta z) \tag{2.63}$$

where in this case ψ represents the dominant transverse electric field component. The periodic dependence on ϕ following $\cos l\phi$ or $\sin l\phi$ gives a mode of radial order l. Hence the fiber supports a finite number of guided modes of the form of Eq. (2.63).

Introducing the solutions given by Eq. (2.63) into Eq. (2.61) results in a differential equation of the form:

$$\frac{d^2\mathbf{E}}{dr^2} + \frac{1}{r}\frac{d\mathbf{E}}{dr} + \left[(n_1k^2 - \beta^2) - \frac{l^2}{r^2}\right]\mathbf{E} = 0 \tag{2.64}$$

For a step index fiber with a constant refractive index core, Eq. (2.64) is a Bessel differential equation and the solutions are cylinder functions. In the core region the solutions are Bessel functions denoted by J_l. A graph of these gradually damped oscillatory functions (with respect to r) is shown in Figure 2.16(a). It may be noted

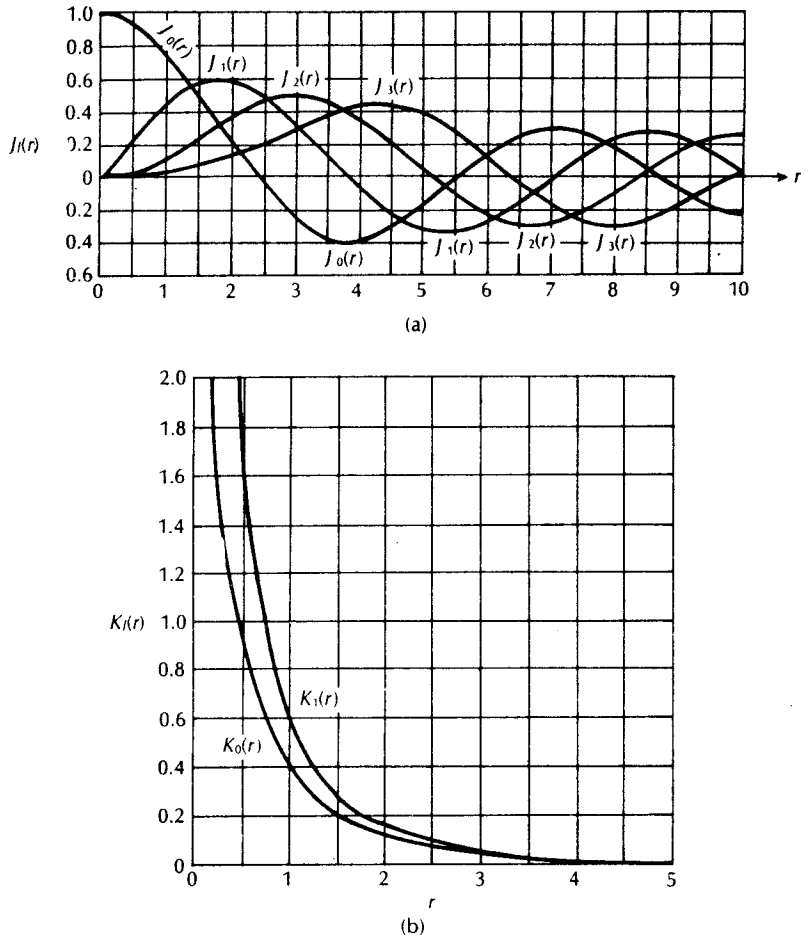

Figure 2.16 (a) Variation of the Bessel function $J_l(r)$ for $l = 0, 1, 2, 3$ (first four orders), plotted against r. (b) Graph of the modified Bessel function $K_l(r)$ against r for $l = 0, 1$.

that the field is finite at $r = 0$ and may be represented by the zero order Bessel function J_0. However, the field vanishes as r goes to infinity and the solutions in the cladding are therefore modified Bessel functions denoted by K_l. These modified functions decay exponentially with respect to r, as illustrated in Figure 2.16(b). The electric field may therefore be given by:

$$\begin{aligned} \mathbf{E}(r) &= GJ_l(UR) && \text{for} \quad R < 1 \text{ (core)} \\ &= GJ_l(U)\frac{K_l(WR)}{K_l(W)} && \text{for} \quad R > 1 \text{ (cladding)} \end{aligned} \tag{2.65}$$

where G is the amplitude coefficient and $R = r/a$ is the normalized radial coordinate when a is the radius of the fiber core; U and W which are the eigenvalues in the core and cladding respectively,* are defined as [Ref. 17]:

$$U = a(n_1^2k^2 - \beta^2)^{\frac{1}{2}} \tag{2.66}$$

$$W = a(\beta^2 - n_2^2k^2)^{\frac{1}{2}} \tag{2.67}$$

The sum of the squares of U and W defines a very useful quantity [Ref. 18] which is usually referred to as the normalized frequency† V where

$$V = (U^2 + W^2)^{\frac{1}{2}} = ka(n_1^2 - n_2^2)^{\frac{1}{2}} \tag{2.68}$$

It may be observed that the commonly used symbol for this parameter is the same as that normally adopted for voltage. However, within this chapter there should be no confusion over this point. Furthermore, using Eqs. (2.8) and (2.10) the normalized frequency may be expressed in terms of the numerical aperture NA and the relative refractive index difference Δ, respectively, as:

$$V = \frac{2\pi}{\lambda} a(NA) \tag{2.69}$$

$$V = \frac{2\pi}{\lambda} an_1(2\Delta)^{\frac{1}{2}} \tag{2.70}$$

The normalized frequency is a dimensionless parameter and hence is also sometimes simply called the V number or value of the fiber. It combines in a very useful manner the information about three important design variables for the fiber: namely, the core radius a, the relative refractive index difference Δ and the operating wavelength λ.

* U is also referred to as the radial phase parameter or the radial propagation constant, whereas W is known as the cladding decay parameter [Ref. 19].

† When used in the context of the planar waveguide, V is sometimes known as the normalized film thickness as it relates to the thickness of the guide layer (see Section 10.5.1).

It is also possible to define the normalized propagation constant b for a fiber in terms of the parameters of Eq. (2.68) so that:

$$b = 1 - \frac{U^2}{V^2} = \frac{(\beta/k)^2 - n_2^2}{n_1^2 - n_2^2}$$

$$= \frac{(\beta/k)^2 - n_2^2}{2n_1^2\Delta} \tag{2.71}$$

Referring to the expression for the guided modes given in Eq. (2.62), the limits of β are n_2k and n_1k, hence b must lie between 0 and 1.

In the weak guidance approximation the field matching conditions at the boundary require continuity of the transverse and tangential electrical field components at the core–cladding interface (at $r = a$). Therefore, using the Bessel function relations outlined previously, an eigenvalue equation for the LP modes may be written in the following form [Ref. 18]:

$$U\frac{J_{l\pm1}(U)}{J_l(U)} = \pm W\frac{K_{l\pm1}(W)}{K_l(W)} \tag{2.72}$$

Solving Eq. (2.72) with Eqs. (2.66) and (2.67) allows the eigenvalue U and hence β to be calculated as a function of the normalized frequency. In this way the propagation characteristics of the various modes, and their dependence on the optical wavelength and the fiber parameters may be determined.

Considering the limit of mode propagation when $\beta = n_2k$, then the mode phase velocity is equal to the velocity of light in the cladding and the mode is no longer properly guided. In this case the mode is said to be cut off and the eigenvalue W = 0 (Eq. 2.67). Unguided or radiation modes have frequencies below cutoff where $\beta < kn_2$, and hence W is imaginary. Nevertheless, wave propagation does not cease abruptly below cutoff. Modes exist where $\beta < kn_2$ but the difference is very small, such that some of the energy loss due to radiation is prevented by an angular momentum barrier [Ref. 21] formed near the core–cladding interface. Solutions of the wave equation giving these states are called leaky modes, and often behave as very lossy guided modes rather than radiation modes. Alternatively, as β is increased above n_2k, less power is propagated in the cladding until at $\beta = n_1k$ all the power is confined to the fiber core. As indicated previously, this range of values for β signifies the guided modes of the fiber.

The lower order modes obtained in a cylindrical homogeneous core waveguide are shown in Figure 2.17 [Ref. 16]. Both the LP notation and the corresponding traditional HE, EH, TE and TM mode notations are indicated. In addition, the Bessel functions J_0 and J_1 are plotted against the normalized frequency and where they cross the zero gives the cutoff point for the various modes. Hence, the cutoff point for a particular mode corresponds to a distinctive value of the normalized frequency (where $V = V_c$) for the fiber. It may be observed from Figure 2.17 that the value of V_c is different for different modes. For example, the first zero crossing J_1 occurs when the normalized frequency is 0 and this corresponds to the cutoff for

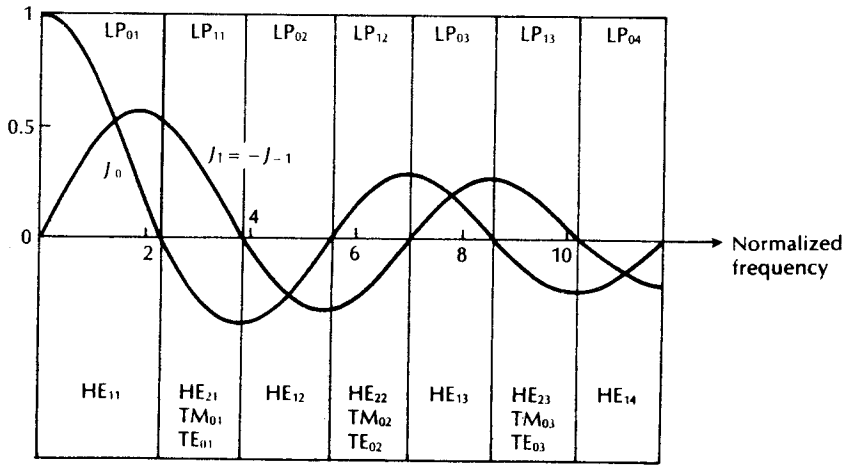

Figure 2.17 The allowed regions for the LP modes of order $l = 0, 1$ against normalized frequency (V) for a circular optical waveguide with a constant refractive index core (step index fiber). Reproduced with permission from D. Gloge. *Appl. Opt.*, **10**, p. 2552, 1971.

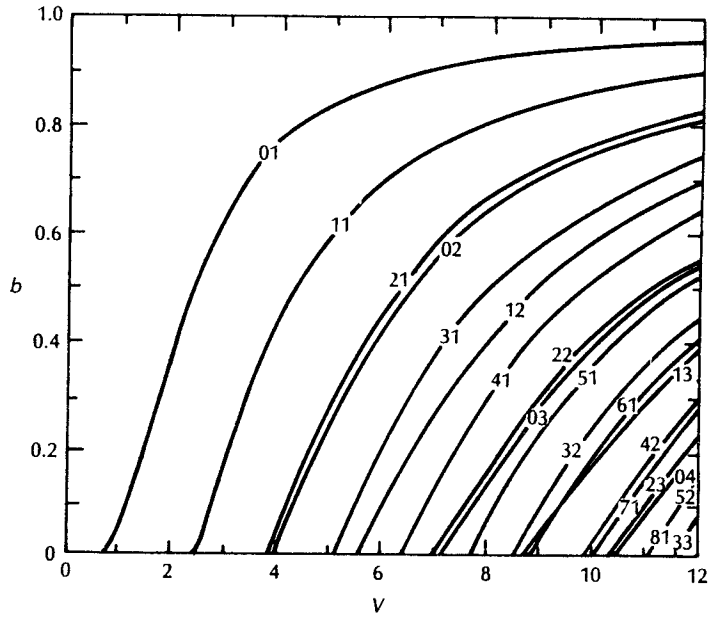

Figure 2.18 The normalized propagation constant b as a function of normalized frequency V for a number of LP modes. Reproduced with permission from D. Gloge. *Appl. Opt.*, **10**, p. 2552, 1971.

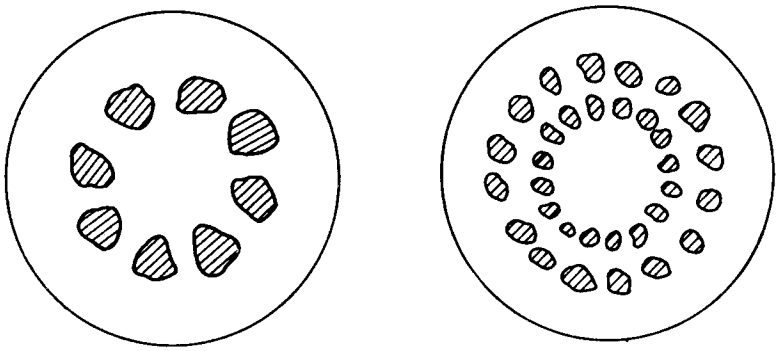

Figure 2.19 Sketches of fiber cross sections illustrating the distinctive light intensity distributions (mode patterns) generated by propagation of individual linearly polarized modes.

the LP_{01} mode. However, the first zero crossing for J_0 is when the normalized frequency is 2.405, giving a cutoff value V_c of 2.405 for the LP_{11} mode. Similarly, the second zero of J_1 corresponds to a normalized frequency of 3.83, giving a cutoff value V_c for the LP_{02} mode of 3.83. It is therefore apparent that fibers may be produced with particular values of normalized frequency which allow only certain modes to propagate. This is further illustrated in Figure 2.18 [Ref. 16] which shows the normalized propagation constant b for a number of LP modes as a function of V. It may be observed that the cutoff value of normalized frequency V_c which occurs when $\beta = n_2k$ corresponds to $b = 0$.

The propagation of particular modes within a fiber may also be confirmed through visual analysis. The electric field distribution of different modes gives similar distributions of light intensity within the fiber core. These waveguide patterns (often called mode patterns) may give an indication of the predominant modes propagating in the fiber. The field intensity distributions for the three lower order LP modes were shown in Figure 2.15. In Figure 2.19 we illustrate the mode patterns for two higher order LP modes. However, unless the fiber is designed for the propagation of a particular mode it is likely that the superposition of many modes will result in no distinctive pattern.

2.4.2 Mode coupling

We have thus far considered the propagation aspects of perfect dielectric waveguides. However, waveguide perturbations such as deviations of the fiber axis from straightness, variations in the core diameter, irregularities at the core–cladding interface and refractive index variations may change the propagation characteristics of the fiber. These will have the effect of coupling energy travelling in one mode to another depending on the specific perturbation.

Ray theory aids the understanding of this phenomenon, as shown in Figure 2.20, which illustrates two types of perturbation. It may be observed that in both cases the ray no longer maintains the same angle with the axis. In electromagnetic wave theory this corresponds to a change in the propagating mode for the light. Thus individual modes do not normally propagate throughout the length of the fiber without large energy transfers to adjacent modes, even when the fiber is exceptionally good quality and is not strained or bent by its surroundings. This mode conversion is known as mode coupling or mixing. It is usually analysed using coupled mode equations which can be obtained directly from Maxwell's equations. However, the theory is beyond the scope of this text and the reader is directed to Ref. 17 for a comprehensive treatment. Mode coupling affects the transmission properties of fibers in several important ways, a major one being in relation to the dispersive properties of fibers over long distances. This is pursued further in Sections 3.8–3.11.

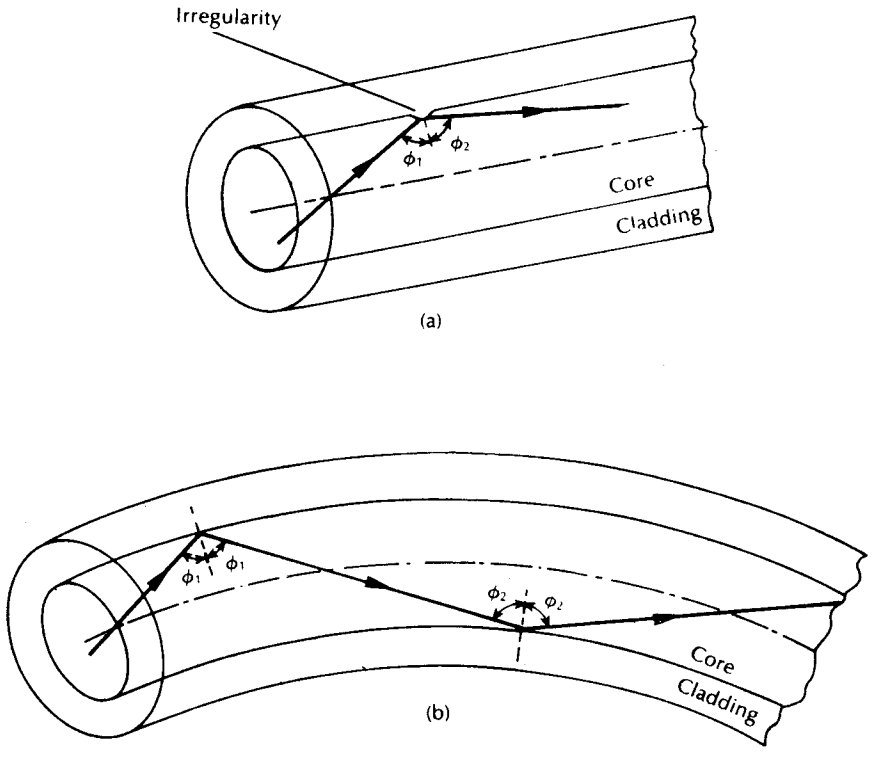

Figure 2.20 Ray theory illustrations showing two of the possible fiber perturbations which give mode coupling: (a) irregularity at the core–cladding interface; (b) fiber bend.

2.4.3 Step index fibers

The optical fiber considered in the preceding sections with a core of constant refractive index n_1 and a cladding of a slightly lower refractive index n_2 is known as step index fiber. This is because the refractive index profile for this type of fiber makes a step change at the core–cladding interface, as indicated in Figure 2.21, which illustrates the two major types of step index fiber. The refractive index profile may be defined as:

$$n(r) = \begin{cases} n_1 & r < a \quad \text{(core)} \\ n_2 & r \geqslant a \quad \text{(cladding)} \end{cases} \tag{2.73}$$

in both cases.

Figure 2.21(a) shows a multimode step index fiber with a core diameter of around 50 μm or greater, which is large enough to allow the propagation of many modes within the fiber core. This is illustrated in Figure 2.21(a) by the many different possible ray paths through the fiber. Figure 2.21(b) shows a single-mode or monomode step index fiber which allows the propagation of only one transverse electromagnetic mode (typically HE_{11}), and hence the core diameter must be of the order of 2 to 10 μm. The propagation of a single mode is illustrated in

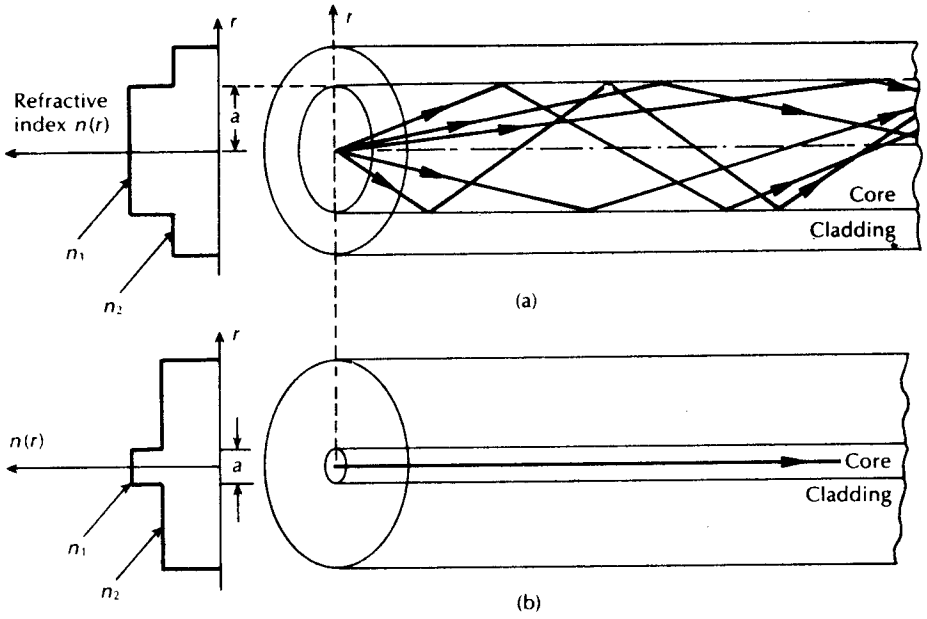

Figure 2.21 The refractive index profile and ray transmission in step index fibers: (a) multimode step index fiber; (b) single-mode step index fiber.

Figure 2.21(b) as corresponding to a single ray path only (usually shown as the axia ray) through the fiber.

The single-mode step index fiber has the distinct advantage of low intermod dispersion (broadening of transmitted light pulses), as only one mode is transmitted, whereas with multimode step index fiber considerable dispersion may occur due to the differing group velocities of the propagating modes (see Section 3.10). This in turn restricts the maximum bandwidth attainable with multimode step index fibers, especially when compared with single-mode fibers. However, for lower bandwidth applications multimode fibers have several advantages over single-mode fibers. These are:

(a) the use of spatially incoherent optical sources (e.g. most light emitting diodes) which cannot be efficiently coupled to single-mode fibers;
(b) larger numerical apertures, as well as core diameters, facilitating easier coupling to optical sources;
(c) lower tolerance requirements on fiber connectors.

Multimode step index fibers allow the propagation of a finite number of guided modes along the channel. The number of guided modes is dependent upon the physical parameters (i.e. relative refractive index difference, core radius) of the fiber and the wavelengths of the transmitted light which are included in the normalized frequency V for the fiber. It was indicated in Section 2.4.1 that there is a cutoff value of normalized frequency V_c for guided modes below which they cannot exist. However, mode propagation does not entirely cease below cutoff. Modes may propagate as unguided or leaky modes wnich can travel considerable distances along the fiber. Nevertheless, it is the guided modes which are of paramount importance in optical fiber communications as these are confined to the fiber over its full length. It can be shown [Ref. 16] that the total number of guided modes or mode volume M_s for a step index fiber is related to the V value for the fiber by the approximate expression

$$M_s \simeq \frac{V^2}{2} \tag{2.74}$$

which allows an estimate of the number of guided modes propagating in a particular multimode step index fiber.

Example 2.4

A multimode step index fiber with a core diameter of 80 μm and a relative index difference of 1.5% is operating at a wavelength of 0.85 μm. If the core refractive index is 1.48, estimate: (a) the normalized frequency for the fiber; (b) the number of guided modes.

Solution: (a) The normalized frequency may be obtained from Eq. (2.70) where:

$$V = \frac{2\pi}{\lambda} a n_1 (2\Delta)^{\frac{1}{2}} = \frac{2\pi \times 40 \times 10^{-6} \times 1.48}{0.85 \times 10^{-6}} (2 \times 0.015)^{\frac{1}{2}} = 75.8$$

(b) The total number of guided modes is given by Eq. (2.74) as:

$$M_s \simeq \frac{V^2}{2} = \frac{5745.6}{2}$$

$$= 2873$$

Hence this fiber has a V number of approximately 76, giving nearly 3000 guided modes.

Therefore, as illustrated in Example 2.4, the optical power is launched into a large number of guided modes, each having different spatial field distributions, propagation constants, etc. In an ideal multimode step index fiber with properties (i.e. relative index difference, core diameter) which are independent of distance, there is no mode coupling, and the optical power launched into a particular mode remains in that mode and travels independently of the power launched into the other guided modes. Also, the majority of these guided modes operate far from cutoff, and are well confined to the fiber core [Ref. 16]. Thus most of the optical power is carried in the core region and not in the cladding. The properties of the cladding (e.g. thickness) do not therefore significantly affect the propagation of these modes.

2.4.4 Graded index fibers

Graded index fibers do not have a constant refractive index in the core* but a decreasing core index $n(r)$ with radial distance from a maximum value of n_1 at the axis to a constant value n_2 beyond the core radius a in the cladding. This index variation may be represented as:

$$n(r) = \begin{cases} n_1(1 - 2\Delta(r/a)^{\alpha})^{\frac{1}{2}} & r < a \quad \text{(core)} \\ n_1(1 - 2\Delta)^{\frac{1}{2}} = n_2 & r \geqslant a \quad \text{(cladding)} \end{cases} \tag{2.75}$$

where Δ is the relative refractive index difference and α is the profile parameter which gives the characteristic refractive index profile of the fiber core. Equation (2.75) which is a convenient method of expressing the refractive index profile of the fiber core as a variation of α allows representation of the step index profile when $\alpha = \infty$, a parabolic profile when $\alpha = 2$ and a triangular profile when $\alpha = 1$. This range of refractive index profiles is illustrated in Figure 2.22.

* Graded index fibers are therefore sometimes referred to as inhomogeneous core fibers.

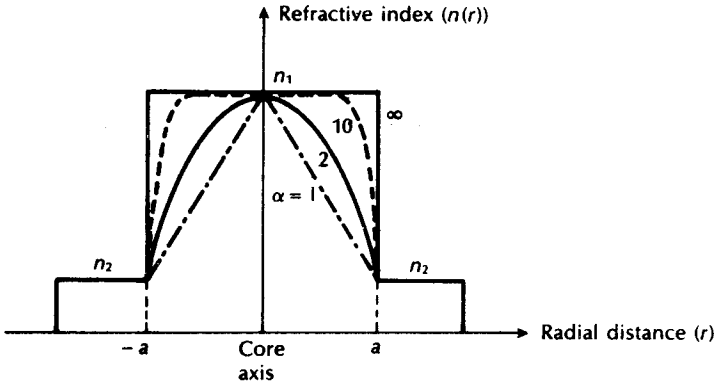

Figure 2.22 Possible fiber refractive index profiles for different values of α (given in Eq. (2.75)).

The graded index profiles which at present produce the best results for multimode optical propagation have a near parabolic refractive index profile core with $\alpha \approx 2$. Fibers with such core index profiles are well established and consequently when the term 'graded index' is used without qualification it usually refers to a fiber with this profile. For this reason in this section we consider the waveguiding properties of graded index fiber with a parabolic refractive index profile core.

A multimode graded index fiber with a parabolic index profile core is illustrated in Figure 2.23. It may be observed that the meridional rays shown appear to follow curved paths through the fiber core. Using the concepts of geometric optics, the gradual decrease in refractive index from the centre of the core creates many refractions of the rays as they are effectively incident on a large number of high to low index interfaces. This mechanism is illustrated in Figure 2.24 where a ray is

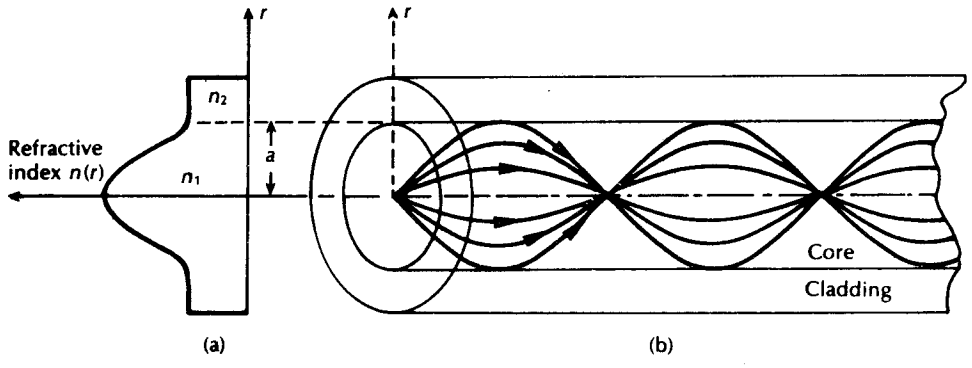

Figure 2.23 The refractive index profile and ray transmission in a multimode graded index fiber.

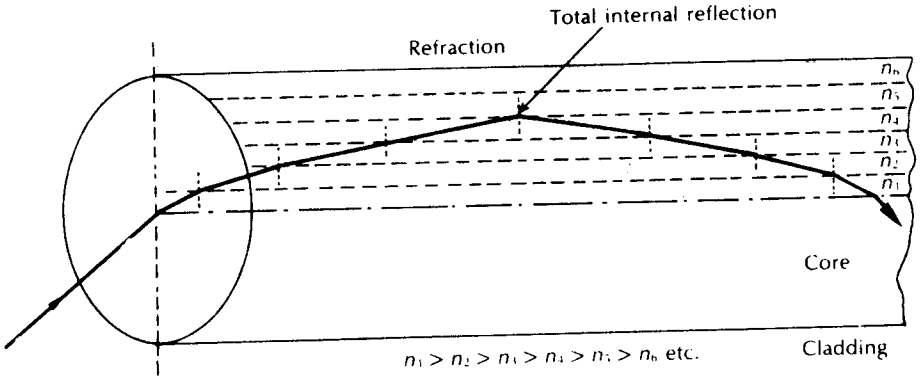

Figure 2.24 An expanded ray diagram showing refraction at the various high to low index interfaces within a graded index fiber, giving an overall curved ray path.

shown to be gradually curved, with an ever-increasing angle of incidence, until the conditions for total internal reflection are met, and the ray travels back toward the core axis, again being continuously refracted.

Multimode graded index fibers exhibit far less intermodal dispersion (see Section 3.10.2) than multimode step index fibers due to their refractive index profile. Although many different modes are excited in the graded index fiber, the different group velocities of the modes tend to be normalized by the index grading. Again considering ray theory, the rays travelling close to the fiber axis have shorter paths when compared with rays which travel into the outer regions of the core. However the near axial rays are transmitted through a region of higher refractive index and therefore travel with a lower velocity than the more extreme rays. This compensates for the shorter path lengths and reduces dispersion in the fiber. A similar situation exists for skew rays which follow longer helical paths, as illustrated in Figure 2.25. These travel for the most part in the lower index region at greater speeds, thus giving the same mechanism of mode transit time equalization. Hence, multimode graded index fibers with parabolic or near parabolic index profile cores have

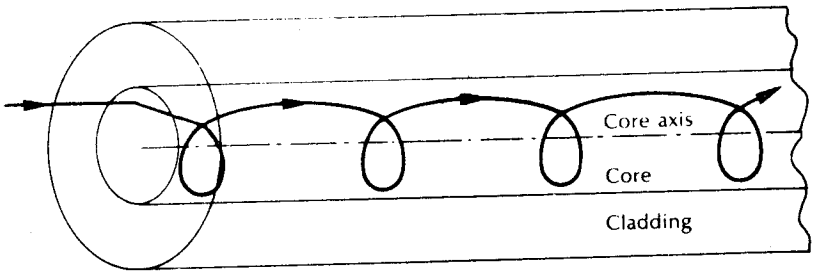

Figure 2.25 A helical skew ray path within a graded index fiber.

transmission bandwidths which may be orders of magnitude greater than multimode step index fiber bandwidths. Consequently, although they are not capable of the bandwidths attainable with single-mode fibers, such multimode graded index fibers have the advantage of large core diameters (greater than 30 μm) coupled with bandwidths suitable for long distance communication.

The parameters defined for step index fibers (i.e. NA, Δ, V) may be applied to graded index fibers and give a comparison between the two fiber types. However, it must be noted that for graded index fibers the situation is more complicated since the numerical aperture is a function of the radial distance from the fiber axis. Graded index fibers, therefore, accept less light than corresponding step index fibers with the same relative refractive index difference.

Electromagnetic mode theory may also be utilized with the graded profiles. Approximate field solutions of the same order as geometric optics are often obtained employing the WKB method from quantum mechanics after Wentzel, Kramers and Brillouin [Ref. 22]. Using the WKB method modal solutions of the guided wave are achieved by expressing the field in the form.

$$E_x = \tfrac{1}{2}[G_1(r)\exp[\mathrm{j}S(r)] + G_2(r)\exp[-\mathrm{j}S(r)]]\begin{pmatrix}\cos l\phi\\ \sin l\phi\end{pmatrix}\exp(\mathrm{j}\beta z) \qquad (2.76)$$

where G and S are assumed to be real functions of the radial distance r.

Substitution of Eq. (2.76) into the scalar wave equation of the form given by Eq. (2.61) (in which the constant refractive index of the fiber core n_1 is replaced by $n(r)$) and neglecting the second derivative of $G_i(r)$ with respect to r provides approximate solutions for the amplitude function $G_i(r)$ and the phase function $S(r)$. It may be observed from the ray diagram shown in Figure 2.23 that a light ray propagating in a graded index fiber does not necessarily reach every point within the fiber core. The ray is contained within two cylindrical caustic surfaces and for most rays a caustic does not coincide with the core–cladding interface. Hence the caustics define the classical turning points of the light ray within the graded fiber core. These turning points defined by the two caustics may be designated as occurring at $r = r_1$ and $r = r_2$.

The result of the WKB approximation yields an oscillatory field in the region $r_1 < r < r_2$ between the caustics where:

$$G_1(r) = G_2(r) = D/[(n^2(r)k^2 - \beta^2)r^2 - l^2]^{\frac{1}{2}} \qquad (2.77)$$

(where D is an amplitude coefficient) and

$$S(r) = \int_{r_1}^{r_2} [(n^2(r)k^2 - \beta^2)r^2 - l^2]^{\frac{1}{2}}\frac{\mathrm{d}r}{r} - \frac{\pi}{4} \qquad (2.78)$$

Outside the interval $r_1 < r < r_2$ the field solution must have an evanescent form. In the region inside the inner caustic defined by $r < r_1$ and assuming r_1 is not too close to $r = 0$, the field decays towards the fiber axis giving:

$$G_1(r) = D\exp(\mathrm{j}mx)/[l^2 - (n^2(r)k^2 - \beta^2)r^2]^{\frac{1}{2}} \qquad (2.79)$$

$$G_2(r) = 0 \qquad (2.80)$$

where the integer m is the radial mode number and

$$S(r) = \mathrm{j} \int_{r}^{r_1} [l^2 - (n^2(r)k^2 - \beta^2)r^2]^{\frac{1}{2}} \frac{\mathrm{d}r}{r} \tag{2.81}$$

Also outside the outer caustic in the region $r > r_2$, the field decays away from the fiber axis and is described by the equations:

$$G_1(r) = D \exp(\mathrm{j}mx)/[l^2 - (n^2(r)k^2 - \beta^2)r^2]^{\frac{1}{4}} \tag{2.82}$$

$$G_2(r) = 0 \tag{2.83}$$

$$S(r) = \mathrm{j} \int_{r_2}^{r} [l^2 - (n^2(r)k^2 - \beta^2)r^2]^{\frac{1}{2}} \frac{\mathrm{d}r}{r} \tag{2.84}$$

The WKB method does not initially provide valid solutions of the wave equation in the vicinity of the turning points. Fortunately, this may be amended by replacing the actual refractive index profile by a linear approximation at the location of the caustics. The solutions at the turning points can then be expressed in terms of Hankel functions of the first and second kind of order $\frac{1}{3}$ [Ref. 23]. This facilitates the joining together of the two separate solutions described previously for inside and outside the interval $r_1 < r < r_2$. Thus the WKB theory provides an approximate eigenvalue equation for the propagation constant β of the guided modes which cannot be determined using ray theory. The WKB eigenvalue equation of which β is a solution is given by [Ref. 23]:

$$\int_{r_1}^{r_2} [(n^2(r)k^2 - \beta^2)r^2 - l^2]^{\frac{1}{2}} \frac{\mathrm{d}r}{r} = (2m - 1)\frac{\pi}{2} \tag{2.85}$$

where the radial mode number $m = 1, 2, 3 \ldots$ and determines the number of maxima of the oscillatory field in the radial direction. This eigenvalue equation can only be solved in a closed analytical form for a few simple refractive index profiles. Hence, in most cases it must be solved approximately or with the use of numerical techniques.

Finally the amplitude coefficient D may be expressed in terms of the total optical power P_G within the guided mode. Considering the power carried between the turning points r_1 and r_2 gives a geometric optics approximation of [Ref. 26]:

$$D = \frac{4(\mu_0/\varepsilon_0)^{\frac{1}{4}} P_G^{\frac{1}{2}}}{n_1 \pi a^2 I} \tag{2.86}$$

where

$$I = \int_{r_1/a}^{r_2/a} \frac{x\mathrm{d}x}{[(n^2(ax)k^2 - \beta^2)a^2x^2 - l^2]^{\frac{1}{2}}} \tag{2.87}$$

The properties of the WKB solution may by observed from a graphical representation of the integrand given in Eq. (2.78). This is shown in Figure 2.26, together with the corresponding WKB solution. Figure 2.26 illustrates the functions $(n^2(r)k^2 - \beta^2)$ and (l^2/r^2). The two curves intersect at the turning points $r = r_1$ and $r = r_2$. The oscillatory nature of the WKB solution between the turning points (i.e.

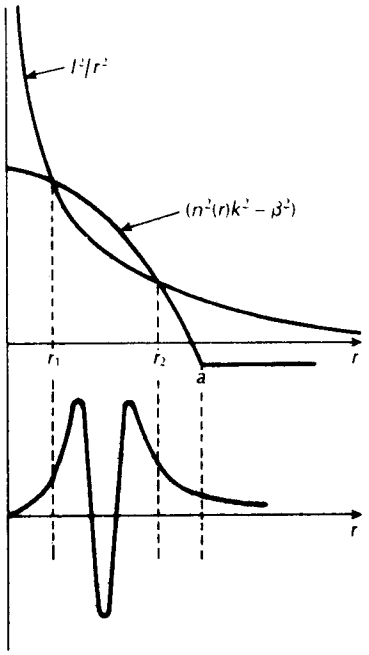

Figure 2.26 Graphical representation of the functions $(n^2(r)k^2 - \beta^2)$ and (l^2/r^2) that are important in the WKB solution and which define the turning points r_1 and r_2. Also shown is an example of the corresponding WKB solution for a guided mode where an oscillatory wave exists in the region between the turning points.

when $l^2/r^2 < n^2(r)k^2 - \beta^2$) which changes into a decaying exponential (evanescent) form outside the interval $r_1 < r < r_2$ (i.e. when $l^2/r^2 > n^2(r)k^2 - \beta^2$) can also be clearly seen.

It may be noted that as the azimuthal mode number l increases, the curve l^2/r^2 moves higher and the region between the two turning points becomes narrower. In addition, even when l is fixed the curve $(n^2(r)k^2 - \beta^2)$ is shifted up and down with alterations in the value of the propagation constant β. Therefore, modes far from cutoff which have large values of β exhibit more closely spaced turning points. As the value of β decreases below n_2k, $(n^2(r)k^2 - \beta^2)$ is no longer negative for large values of r and the guided mode situation depicted in Figure 2.26 changes to one corresponding to Figure 2.27. In this case a third turning point $r = r_3$ is created when at $r = a$ the curve $(n^2(r)k^2 - \beta^2)$ becomes constant, thus allowing the curve (l^2/r^2) to drop below it. Now the field displays an evanescent, exponentially decaying form in the region $r_2 < r < r_3$, as shown in Figure 2.27. Moreover, for $r > r_3$ the field resumes an oscillatory behaviour and therefore carries power away from the fiber core. Unless mode cutoff occurs at $\beta = n_2k$ the guided mode is no

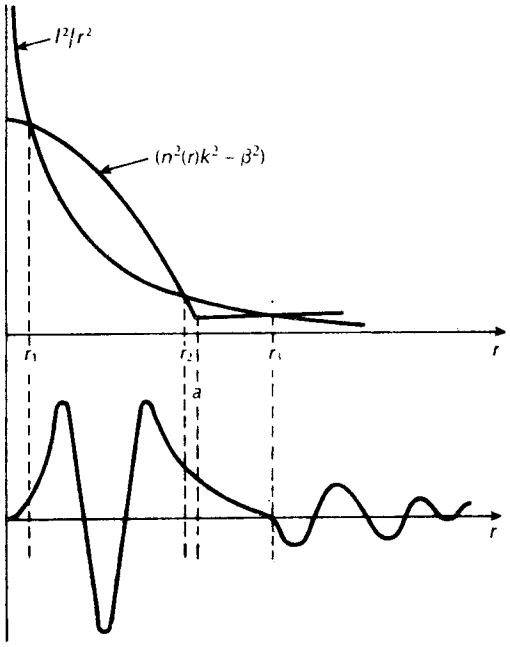

Figure 2.27 Similar graphical representation as that illustrated in Figure 2.26. Here the curve $(n^2(r)k^2 - \beta^2)$ no longer goes negative and a third turning point r_3 occurs. This corresponds to leaky mode solutions in the WKB method.

longer fully contained within the fiber core but loses power through leakage or tunnelling into the cladding. This situation corresponds to the leaky modes mentioned previously in Section 2.4.1.

The WKB method may be used to calculate the propagation constants for the modes in a parabolic refractive index profile core fiber where, following Eq. (2.75):

$$n^2(r) = n_1^2\left(1 - 2\left(\frac{r}{a}\right)^2\Delta\right) \quad \text{for} \quad r < a \tag{2.88}$$

Substitution of Eq. (2.88) into Eq. (2.85) gives:

$$\int_{r_1}^{r_2}\left[n_1^2k^2 - \beta^2 - 2n_1^2k^2\left(\frac{r}{a}\right)^2\Delta - \frac{l^2}{r^2}\right]^{\frac{1}{2}} \mathrm{d}r = (m + \tfrac{1}{2})\pi \tag{2.89}$$

The integral shown in Eq. (2.89) can be evaluated using a change of variable from r to $u = r^2$. The integral obtained may be found in a standard table of indefinite integrals [Ref. 27]. As the square root term in the resulting expression goes to zero at the turning points (i.e. $r = r_1$ and $r = r_2$), then we can write

$$\left[\frac{a(n_1k^2 - \beta^2)}{4n_1k\sqrt{(2\Delta)}} - \frac{l}{2}\right]\pi = (m + \tfrac{1}{2})\pi \tag{2.90}$$

Solving Eq. (2.90) for β^2 gives:

$$\beta^2 = n_1^2 k^2 \left[\frac{1 - 2\sqrt{(2\Delta)}}{n_1 ka} (2m + l + 1) \right] \tag{2.91}$$

It is interesting to note that the solution for the propagation constant for the various modes in a parabolic refractive index core fiber given in Eq. (2.91) is exact even though it was derived from the approximate WKB eigenvalue equation (Eq. 2.85). However, although Eq. (2.91) is an exact solution of the scalar wave equation for an infinitely extended parabolic profile medium, the wave equation is only an approximate representation of Maxwell's equation. Furthermore, practical parabolic refractive index profile core fibers exhibit a truncated parabolic distribution which merges into a constant refractive index at the cladding. Hence Eq. (2.91) is not exact for real fibers.

Equation (2.91) does, however, allow us to consider the mode number plane spanned by the radial and azimuthal mode numbers m and l. This plane is displayed in Figure 2.28, where each mode of the fiber described by a pair of mode numbers is represented as a point in the plane. The mode number plane contains guided, leaky and radiation modes. The mode boundary which separates the guided modes from the leaky and radiation modes is indicated by the solid line in Figure 2.28. It depicts a constant value of β following Eq. (2.91) and occurs when $\beta = n_2 k$. Therefore, all the points in the mode number plane lying below the line $\beta = n_2 k$ are associated with guided modes, whereas the region above the line is occupied by leaky and radiation modes. The concept of the mode plane allows us to count the total number of guided modes within the fiber. For each pair of mode numbers m and l the corresponding mode field can have azimuthal mode dependence cos $l\phi$ or sin $l\phi$ and can exist in two possible polarizations (see Section 3.13). Hence the

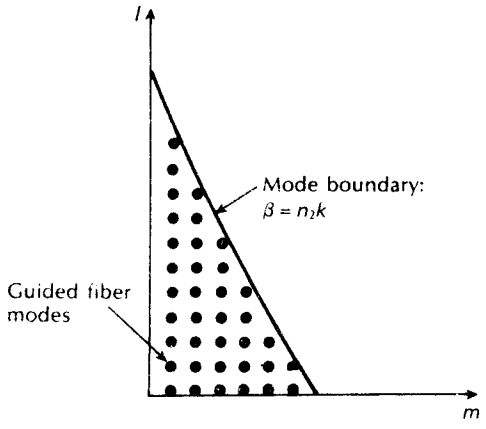

Figure 2.28 The mode number plane illustrating the mode boundary and the guided fiber modes.

modes are said to be fourfold degenerate.* If we define the mode boundary as the function $m = f(l)$, then the total number of guided modes M is given by

$$M = 4 \int_0^{l_{max}} f(l)\, dl \tag{2.92}$$

as each representation point corresponding to four modes occupies an element of unit area in the mode plane. Equation (2.92) allows the derivation of the total number of guided modes or mode volume M_g supported by the graded index fiber. It can be shown [Ref. 23] that:

$$M_g = \left(\frac{\alpha}{\alpha + 2}\right)(n_1 ka)^2 \Delta \tag{2.93}$$

Furthermore, utilizing Eq. (2.70), the normalized frequency V for the fiber when $\Delta \ll 1$ is approximately given by:

$$V = n_1 ka(2\Delta)^{\frac{1}{2}} \tag{2.94}$$

Substituting Eq. (2.94) into Eq. (2.93), we have:

$$M_g \simeq \left(\frac{\alpha}{\alpha + 2}\right)\left(\frac{V^2}{2}\right) \tag{2.95}$$

Hence for a parabolic refractive index profile core fiber ($\alpha = 2$), $M_g \approx V^2/4$, which is half the number supported by a step index fiber ($\alpha = \infty$) with the same V value.

Example 2.5

A graded index fiber has a core with a parabolic refractive index profile which has a diameter of 50 μm. The fiber has a numerical aperture of 0.2. Estimate the total number of guided modes propagating in the fiber when it is operating at a wavelength of 1 μm.

Solution: Using Eq. (2.69), the normalized frequency for the fiber is:

$$V = \frac{2\pi}{\lambda} a(NA) = \frac{2\pi \times 25 \times 10^{-6} \times 0.2}{1 \times 10^{-6}}$$

$$= 31.4$$

The mode volume may be obtained from Eq. (2.95) where for a parabolic profile:

$$M_g \simeq \frac{V^2}{4} = \frac{986}{4} = 247$$

Hence the fiber supports approximately 247 guided modes.

---

* An exception to this are the modes that occur when $l = 0$ which are only doubly degenerate as $\cos l\phi$ becomes unity and $\sin l\phi$ vanishes. However, these modes represent only a small minority and therefore may be neglected.

2.5 Single-mode fibers

The advantage of the propagation of a single mode within an optical fiber is that the signal dispersion caused by the delay differences, between different modes in a multimode fiber may be avoided (see Section 3.10). Multimode step index fibers do not lend themselves to the propagation of a single mode due to the difficulties of maintaining single-mode operation within the fiber when mode conversion (i.e. coupling) to other guided modes takes place at both input mismatches and fiber imperfections. Hence, for the transmission of a single mode the fiber must be designed to allow propagation of only one mode, whilst all other modes are attenuated by leakage or absorption.

Following the preceding discussion of multimode fibers, this may be achieved through choice of a suitable normalized frequency for the fiber. For single-mode operation, only the fundamental LP_{01} mode can exist. Hence the limit of single-mode operation depends on the lower limit of guided propagation for the LP_{11} mode. The cutoff normalized frequency for the LP_{11} mode in step index fibers occurs at $V_c = 2.405$ (see Section 2.4.1). Thus single-mode propagation of the LP_{01} mode in step index fibers is possible over the range:

$$0 \leqslant V < 2.405 \tag{2.96}$$

as there is no cutoff for the fundamental mode. It must be noted that there are in fact two modes with orthogonal polarization over this range, and the term singl mode applies to propagation of light of a particular polarization. Also, it is apparent that the normalized frequency for the fiber may be adjusted to within the range given in Eq. (2.96) by reduction of the core radius, and possibly the relative refractive index difference following Eq. (2.70) which, for single-mode fibers, is usually less than 1%.

Example 2.6

Estimate the maximum core diameter for an optical fiber with the same relative refractive index difference (1.5%) and core refractive index (1.48) as the fiber given in Example 2.4 in order that it may be suitable for single-mode operation. It may be assumed that the fiber is operating at the same wavelength (0.85 μm). Further, estimate the new maximum core diameter for single-mode operation when the relative refractive index difference is reduced by a factor of 10.

Solution: Considering the relationship given in Eq. (2.96), the maximum V value for a fiber which gives single-mode operation is 2.4. Hence, from Eq. (2.70) the core radius a is:

$$a = \frac{V\lambda}{2\pi n_1 (2\Delta)^{\frac{1}{2}}} = \frac{2.4 \times 0.85 \times 10^{-6}}{2\pi \times 1.48 \times (0.03)^{\frac{1}{2}}}$$

$$= 1.3\ \mu\text{m}$$

Therefore the maximum core diameter for single-mode operation is approximately 2.6 μm.

Reducing the relative refractive index difference by a factor of 10 and again using Eq. (2.70) gives:

$$a = \frac{2.4 \times 0.85 \times 10^{-6}}{2\pi \times 1.48 \times (0.003)^{\frac{1}{2}}} = 4.0\ \mu\text{m}.$$

Hence the maximum core diameter for single-mode operation is now approximately 8 μm.

It is clear from Example 2.6 that in order to obtain single-mode operation with a maximum V number of 2.4 the single-mode fiber must have a much smaller core diameter than the equivalent multimode step index fiber (in this case by a factor of 32). However, it is possible to achieve single-mode operation with a slightly larger core diameter, albeit still much less than the diameter of multimode step index fiber, by reducing the relative refractive index difference of the fiber.* Both these factors create difficulties with single-mode fibers. The small core diameters pose problems with launching light into the fiber and with field jointing, and the reduced relative refractive index difference presents difficulties in the fiber fabrication process.

Graded index fibers may also be designed for single-mode operation and some specialist fiber designs do adopt such non-step index profiles (see Section 3.12). However, it may be shown [Ref. 28] that the cutoff value of normalized frequency V_c to support a single mode in a graded index fiber is given by:

$$V_c = 2.405(1 + 2/\alpha)^{\frac{1}{2}} \tag{2.97}$$

Therefore, as in the step index case, it is possible to determine the fiber parameters which give single-mode operation.

Example 2.7

A graded index fiber with a parabolic refractive index profile core has a refractive index at the core axis of 1.5 and a relative index difference of 1%. Estimate the maximum possible core diameter which allows single-mode operation at a wavelength of 1.3 μm.

Solution: Using Eq. (2.97) the maximum value of normalized frequency for single-mode operation is

$$V = 2.4(1 + 2/\alpha)^{\frac{1}{2}} = 2.4(1 + 2/2)^{\frac{1}{2}}$$
$$= 2.4\sqrt{2}$$

* Practical values for single-mode step index fiber designed for operation at a wavelength of 1.3 μm are $\Delta = 0.3\%$, giving $2a = 8.5\ \mu$m.

The maximum core radius may be obtained from Eq. (2.70) where:

$$a = \frac{V\lambda}{2\pi n_1 (2\Delta)^{\frac{1}{2}}} = \frac{2.4\sqrt{2} \times 1.3 \times 10^{-6}}{2\pi \times 1.5 \times (0.02)^{\frac{1}{2}}}$$

$$= 3.3\ \mu\text{m}$$

Hence the maximum core diameter which allows single-mode operation is approximately 6.6 μm.

It may be noted that the critical value of normalized frequency for the parabolic profile graded index fiber is increased by a factor of $\sqrt{2}$ on the step index case. This gives a core diameter increased by a similar factor for the graded index fiber over a step index fiber with the equivalent core refractive index (equivalent to the core axis index), and the same relative refractive index difference.

The maximum V number which permits single-mode operation can be increased still further when a graded index fiber with a triangular profile is employed. It is apparent from Eq. (2.97) that the increase in this case is by a factor of $\sqrt{3}$ over a comparable step index fiber. Hence, significantly larger core diameter single-mode fibers may be produced utilizing this index profile. Such advanced refractive index profiles, which came under serious investigation in the early 1980s [Ref. 29], have now been adopted, particularly in the area of dispersion modified fiber design (see Section 3.12).

A further problem with single-mode fibers with low relative refractive index differences and low V values is that the electromagnetic field associated with the LP_{10} mode extends appreciably into the cladding. For instance, with V values less than 1.4, over half the modal power propagates in the cladding [Ref. 21]. Thus the exponentially decaying evanescent field may extend significant distances into the cladding. It is therefore essential that the cladding is of a suitable thickness, and has low absorption and scattering losses in order to reduce attenuation of the mode. Estimates [Ref. 30] show that the necessary cladding thickness is of the order of 50 μm to avoid prohibitive losses (greater than 1 dB km^{-1}) in single-mode fibers, especially when additional losses resulting from microbending (see Section 4.8.1) are taken into account. Therefore, the total fiber cross section for single-mode fibers is of a comparable size to multimode fibers.

Another approach to single-mode fiber design which allows the V value to be increased above 2.405 is the W fiber [Ref. 32]. The refractive index profile for this fiber is illustrated in Figure 2.29 where two cladding regions may be observed. Use of such two step cladding allows the loss threshold between the desirable and undesirable modes to be substantially increased. The fundamental mode will be fully supported with small cladding loss when its propagation constant lies in the range $kn_3 < \beta < kn_1$.

If the undesirable higher order modes which are excited or converted to have values of propagation constant $\beta < kn_3$, they will leak through the barrier layer

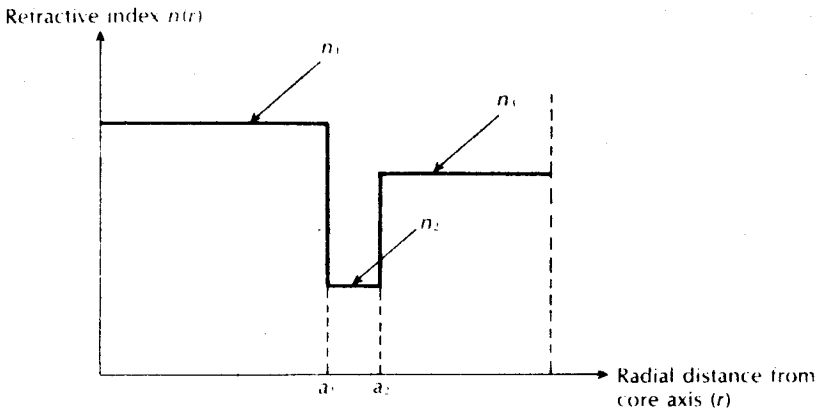

Figure 2.29 The refractive index profile for a single-mode *W* fiber.

between a_1 and a_2 (Figure 2.29) into the outer cladding region n_3. Consequently these modes will lose power by radiation into the lossy surroundings. This design can provide single-mode fibers with larger core diameters than can the conventional single cladding approach which proves useful for easing jointing difficulties; W fibers also tend to give reduced losses at bends in comparison with conventional single-mode fibers.

Although single-mode fibers have only relatively recently emerged (i.e. since 1983) as a viable optical communication medium they have quickly become the dominant and the most widely used fiber type within telecommunications.* Major reasons for this situation are as follows:

1. They currently exhibit the greatest transmission bandwidths and the lowest losses of the fiber transmission media (see Chapter 3).
2. They have a superior transmission quality over other fiber types because of the absence of modal noise (see Section 3.10.3).
3. They offer a substantial upgrade capability (i.e. future proofing) for future wide bandwidth services using either faster optical transmitters and receivers or advanced transmission techniques (e.g. coherent technology, see Chapter 12).
4. They are compatible with the developing integrated optics technology (see Chapter 10).
5. The above (1) to (4) provide a confidence that the installation of single-mode fiber will provide a transmission medium which will have adequate performance such that it will not require replacement over its twenty-plus-year anticipated lifetime.

At present the most commonly used single-mode fibers employ a step index (or near

* Multimode fibers are still finding extensive use within more localized communications (e.g. in data links and local area networks).

step index) profile design and are dispersion optimized (see Section 3.11.2) for operation in the 1.3 μm wavelength region. These fibers are either of a matched-cladding (MC) or a depressed-cladding (DC) design, as illustrated in Figure 2.30. In the conventional MC fibers, the region external to the core has a constant uniform refractive index which is slightly lower than the core region, typically consisting of pure silica. Alternatively when the core region comprises pure silica then the lower index cladding is obtained through fluorine doping. A mode-field diameter (MFD) (see Section 2.5.2) of 10 μm is typical for MC fibers with relative refractive index differences of around 0.3%. However, improved bend loss performance (see Section 3.6) has been achieved in the 1.55 μm wavelength region with reduced MFDs of about 9.5 μm and relative refractive index differences of 0.37%. [Ref. 40].

A more recent experimental MC fiber design employs a segmented core as shown in Figure 2.30(b) [Ref. 41]. Such a structure provides conventional single-mode dispersion optimized performance at wavelengths around 1.3 μm but is multimoded with a few modes (two or three) in the shorter wavelength region around 0.8 μm. The multimode operating region is intended to help relax both the tight tolerances involved when coupling LEDs to such single-mode fibers (see Section 7.3.6) and their connectorization. Thus segmented core fiber of this type could find use in

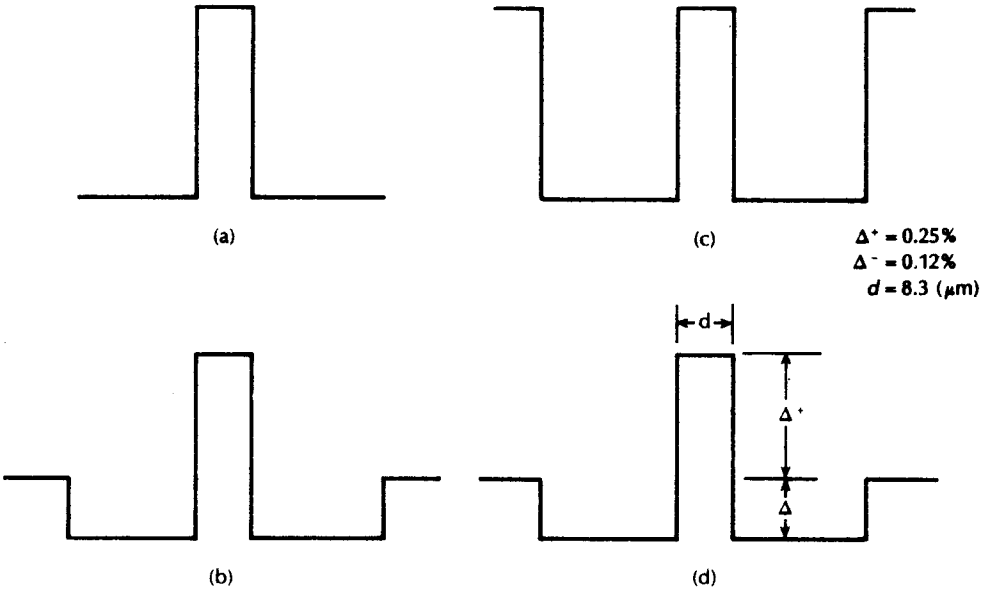

Figure 2.30 Single-mode fiber step index profiles optimized for operation at a wavelength of 1.3 μm: (a) conventional matched-cladding design; (b) segmented core matched-cladding design; (c) depressed-cladding design; (d) profile specifications of a depressed-cladding fiber [Ref. 42].

applications which require an inexpensive initial solution but upgradeability to conventional single-mode fiber performance at the 1.3 μm wavelength in the future.

In the DC fibers shown in Figure 2.30 the cladding region immediately adjacent to the core is of a lower refractive index than that of an outer cladding region. A typical MFD (see Section 2.5.2) of a DC fiber is 9 μm with positive and negative relative refractive index differences of 0.25% and 0.12% (see Figure 2.30(d)) [Ref. 42].

2.5.1 Cutoff wavelength

It may be noted by rearrangement of Eq. (2.70) that single-mode operation only occurs above a theoretical cutoff wavelength λ_c given by:

$$\lambda_c = \frac{2\pi a n_1}{V_c}(2\Delta)^{\frac{1}{2}} \tag{2.98}$$

where V_c is the cutoff normalized frequency. Hence λ_c is the wavelength above which a particular fiber becomes single-moded. Dividing Eq. (2.98) by Eq. (2.70) for the same fiber we obtain the inverse relationship:

$$\frac{\lambda_c}{\lambda} = \frac{V}{V_c} \tag{2.99}$$

Thus for step index fiber where $V_c = 2.405$, the cutoff wavelength is given by [Ref. 43]:

$$\lambda_c = \frac{V\lambda}{2.405} \tag{2.100}$$

An effective cutoff wavelength has been defined by the CCITT* [Ref. 44] which is obtained from a 2 m length of fiber containing a single 14 cm radius loop. This definition was produced because the first higher order LP_{11} mode is strongly affected by fiber length and curvature near cutoff. Recommended cutoff wavelength values for primary coated fiber range from 1.1 to 1.28 μm for single-mode fiber designed for operation in the 1.3 μm wavelength region in order to avoid modal noise and dispersion problems. Moreover, practical transmission systems are generally operated close to the effective cutoff wavelength in order to enhance the fundamental mode confinement, but sufficiently distant from cutoff so that no power is transmitted in the second order LP_{11} mode.

Example 2.8

Determine the cutoff wavelength for a step index fiber to exhibit single-mode operation when the core refractive index and radius are 1.46 and 4.5 μm, respectively, with the relative index difference being 0.25%.

* Recommendation G 652.

Solution: Using Eq. (2.98) with $V_c = 2.405$ gives:

$$\lambda_c = \frac{2\pi a n_1 (2\Delta)^{\frac{1}{2}}}{2.405} = \frac{2\ 4.5 \times 1.46(0.005)^{\frac{1}{2}}}{2.405}\ \mu\text{m}$$

$$= 1.214\ \mu\text{m}$$

$$= 1214\ \text{nm}$$

Hence the fiber is single-moded to a wavelength of 1214 nm.

2.5.2 Mode-field diameter and spot size

Many properties of the fundamental mode are determined by the radial extent of its electromagnetic field including losses at launching and jointing, microbend losses, waveguide dispersion and the width of the radiation pattern. Therefore, the mode-field diameter (MFD) is an important parameter for characterizing single-mode fiber properties which takes into account the wavelength dependent field penetration into the fiber cladding. In this context it is a better measure of the functional properties of single-mode fiber than the core diameter. For step index and graded (near parabolic profile) single-mode fibers operating near the cutoff wavelength λ_c, the field is well approximated by a Gaussian distribution (see Section 2.5.5). In this case the MFD is generally taken as the distance between the opposite $1/e = 0.37$ field amplitude points and the power $1/e^2 = 0.135$ points in relation to the corresponding values on the fiber axis, as shown in Figure 2.31.

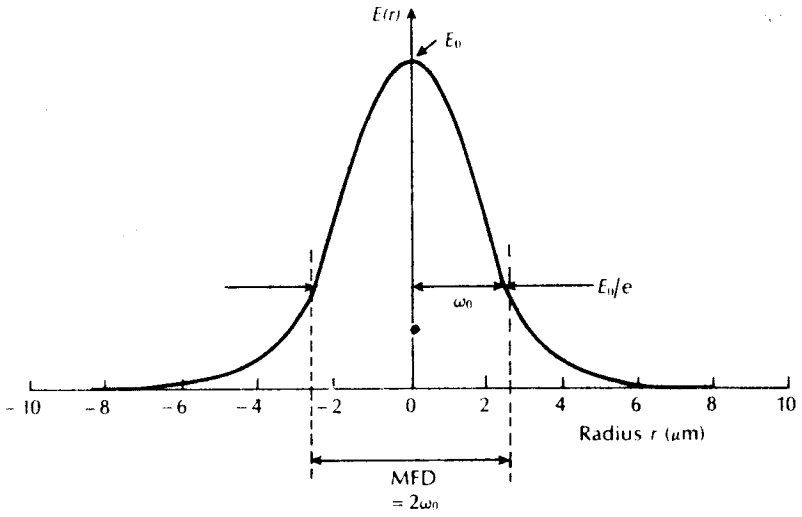

Figure 2.31 Field amplitude distribution $E(r)$ of the fundamental mode in a single-mode fiber illustrating the mode-field diameter (MFD) and spot size (ω_0)

Another parameter which is directly related to the mode-field diameter of a single-mode fiber is the spot size (or mode-field radius) ω_0. Hence $MFD = 2\,\omega_0$, where ω_0 is the nominal half width of the input excitation (see Figure 2.31). The MFD can therefore be regarded as the single-mode analog of the fiber core diameter in multimode fibers [Ref. 45]. However, for many refractive index profiles and at typical operating wavelengths the MFD is slightly larger than the single-mode fiber core diameter.

Often, for real fibers and those with arbitrary refractive index profiles the radial field distribution is not strictly Gaussian and hence alternative techniques have been proposed. However, the problem of defining the MFD and spot size for non-Gaussian field distributions is a difficult one and at least eight definitions exist [Ref. 19]. Nevertheless, a more general definition based on the second moment of the far field and known as the Petermann II definition [Ref. 46] is recommended by the CCITT. Moreover, good agreement has been obtained using this definition for the MFD using different measurement techniques on arbitrary index fibers [Ref. 47].

2.5.3 Effective refractive index

The rate of change of phase of the fundamental LP_{01} mode propagating along a straight fiber is determined by the phase propagation constant β (see Section 2.3.2). It is directly related to the wavelength of the LP_{01} mode λ_{01} by the factor 2π, since β gives the increase in phase angle per unit length. Hence:

$$\beta\lambda_{01} = 2\pi, \text{ or } \lambda_{01} = \frac{2\pi}{\beta} \tag{2.101}$$

Moreover, it is convenient to define an effective refractive index for single-mode fiber, sometimes referred to as a phase index or normalized phase change coefficient [Ref. 48] n_{eff}, by the ratio of the propagation constant of the fundamental mode to that of the vacuum propagation constant:

$$n_{\text{eff}} = \frac{\beta}{k} \tag{2.102}$$

Hence, the wavelength of the fundamental mode λ_{01} is smaller than the vacuum wavelength λ by the factor $1/n_{\text{eff}}$ where:

$$\lambda_{01} = \frac{\lambda}{n_{\text{eff}}} \tag{2.103}$$

It should be noted that the fundamental mode propagates in a medium with a refractive index $n(r)$ which is dependent on the distance r from the fiber axis. The effective refractive index can therefore be considered as an average over the refractive index of this medium [Ref. 19].

Within a normally clad fiber, not depressed-cladded fibers (see Section 2.5), at long wavelengths (i.e. small V values) the mode-field diameter is large compared to the core diameter and hence the electric field extends far into the cladding region.

In this case the propagation constant β will be approximately equal to n_2k (i.e. the cladding wavenumber) and the effective index will be similar to the refractive index of the cladding n_2. Physically, most of the power is transmitted in the cladding material. At short wavelengths, however, the field is concentrated in the core region and the propagation constant β approximates to the maximum wave-number n_1k. Following this discussion, and as indicated previously in Eq. (2.62), then the propagation constant in single-mode fiber varies over the interval $n_2k < \beta < n_1k$. Hence, the effective refractive index will vary over the range $n_2 < n_{\text{eff}} < n_1$.

In addition, a relationship between the effective refractive index and the normalized propagation constant b defined in Eq. (2.71) as:

$$b = \frac{(\beta/k)^2 - n_2^2}{n_1^2 - n_2^2} = \frac{\beta^2 - n_2^2k^2}{n_1k^2 - n_2^2k^2} \tag{2.104}$$

may be obtained. Making use of the mathematical relation, $A^2 - B^2 = (A + B)(A - B)$, Eq. (2.104) can be written in the form:

$$b = \frac{(\beta + n_2k)(\beta - n_2k)}{(n_1k + n_2k)(n_1k - n_2k)} \tag{2.105}$$

However, taking regard of the fact that $\beta \simeq n_1k$, then Eq. (2.105) becomes:

$$b \simeq \frac{\beta - n_2k}{n_1k - n_2k} = \frac{\beta/k - n_2}{n_1 - n_2}$$

Finally, in Eq. (2.102) n_{eff} is equal to β/k, therefore:

$$b \simeq \frac{n_{\text{eff}} - n_2}{n_1 - n_2} \tag{2.106}$$

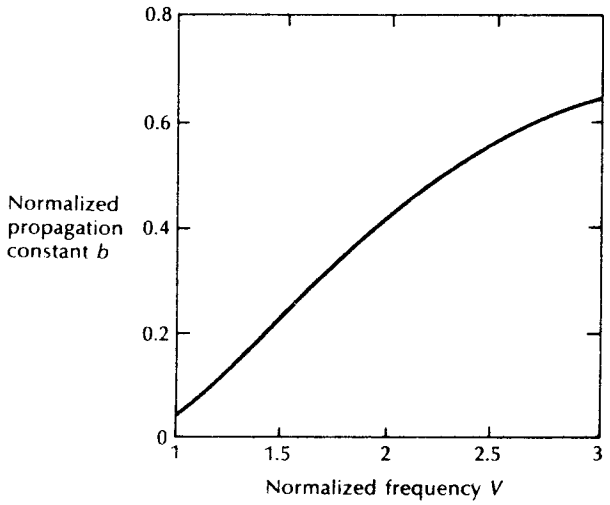

Figure 2.32 The normalized propagation constant (b) of the fundamental mode in a step index fiber shown as a function of the normalized frequency (V).

The dimensionless parameter b which varies between 0 and 1 is particularly useful in the theory of single-mode fibers because the relative refractive index difference is very small giving only a small range for β. Moreover, it allows a simple graphical representation of results to be presented as illustrated by the characteristic shown in Figure 2.32 of the normalized phase constant of β as a function of normalized frequency V in a step index fiber.* It should also be noted that $b(V)$ is a universal function which does not depend explicitly on other fiber parameters.

Example 2.9

Given that a useful approximation for the eigenvalue of the single-mode step index fiber cladding W is [Ref. 43]:

$$W(V) \simeq 1.1428\ \mathrm{V} - 0.9960$$

deduce an approximation for the normalized propagation constant $b(V)$.

Solution: Substituting from Eq. (2.68) into Eq. (2.71), the normalized propagation constant is given by:

$$b(V) = 1 - \frac{(V^2 - W^2)}{V^2} = \frac{W^2}{V^2}$$

Then substitution of the approximation above gives:

$$b(V) \simeq \frac{(1.1428\ \mathrm{V} - 0.9960)^2}{V^2}$$

$$= \left(1.1428 - \frac{0.9960}{V}\right)^2$$

The relative error on this approximation for $b(V)$ is less than 0.2% for $1.5 \leqslant V \leqslant 2.5$ and less than 2% for $1 \leqslant V \leqslant 3$ [Ref. 43].

2.5.4 Group delay and mode delay factor

The transit time or group delay τ_g for a light pulse propagating along a unit length of fiber is the inverse of the group velocity v_g (see Section 2.3.3). Hence:

$$\tau_g = \frac{1}{v_g} = \frac{\mathrm{d}\beta}{\mathrm{d}\omega} = \frac{1}{c}\frac{\mathrm{d}\beta}{\mathrm{d}k} \tag{2.107}$$

The group index of a uniform plane wave propagating in a homogeneous medium

* For step index fibers the eigenvalue U, which determines the radial field distribution in the core, can be obtained from the plot of b versus V because from Eq. (2.71), $U^2 = V^2(1 - b)$.

has been determined following Eq. (2.40) as:

$$N_g = \frac{c}{v_g}$$

However, for a single-mode fiber, it is usual to define an effective group index* N_{ge} [Ref. 48] by:

$$N_{ge} = \frac{c}{v_g} \tag{2.108}$$

where v_g is considered to be the group velocity of the fundamental fiber mode. Hence, the specific group delay of the fundamental fiber mode becomes:

$$\tau_g = \frac{N_{ge}}{c} \tag{2.109}$$

Moreover, the effective group index may be written in terms of the effective refractive index n_{eff} defined in Eq. (2.102) as:

$$N_{ge} = n_{eff} - \lambda \frac{dn_{eff}}{d\lambda} \tag{2.110}$$

It may be noted that Eq. (2.110) is of the same form as the denominator of Eq. (2.40) which gives the relationship between the group index and the refractive index in a transparent medium (planar guide).

Rearranging Eq. (2.71) β may be expressed in terms of the relative index difference Δ and the normalized propagation constant b by the following approximate expression:

$$\beta = k[(n_1^2 - n_2^2)b + n_2^2]^{\frac{1}{2}} \simeq kn_2[1 + b\Delta] \tag{2.111}$$

Furthermore, approximating the relative refractive index difference as $(n_1 - n_2)/n_2$, for a weakly guiding fiber where $\Delta \ll 1$, we can use the approximation [Ref. 16]:

$$\frac{n_1 - n_2}{n_2} \simeq \frac{N_{g1} - N_{g2}}{N_{g2}} \tag{2.112}$$

where N_{g1} and N_{g2} are the group indices for the fiber core and cladding regions respectively. Substituting Eq. (2.111) for β into Eq. (2.107) and using the approximate expression given in Eq. (2.112) we obtain the group delay per unit distance as:

$$\tau_g = \frac{1}{c}\left[N_{g2} + (N_{g1} - N_{g2})\frac{d(Vb)}{dV}\right] \tag{2.113}$$

The dispersive properties of the fiber core and the cladding are often about the same and therefore the wavelength dependence of Δ can be ignored [Ref. 19].

* N_{ge} may also be referred to as the group index of the single-mode waveguide.

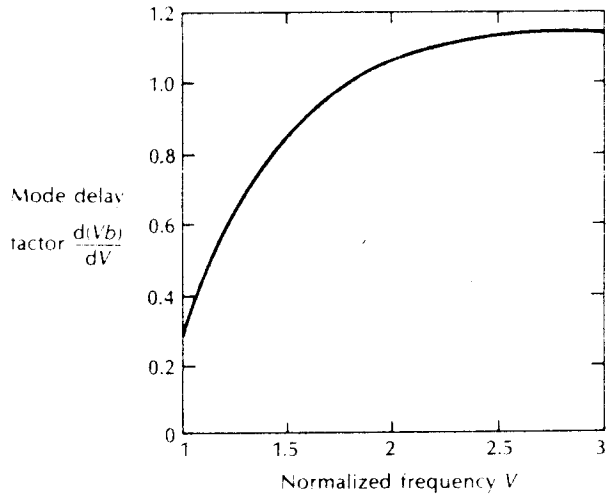

Figure 2.33 The mode delay factor $(d(Vb)/dV)$ for the fundamental mode in a step index fiber shown as a function of normalized frequency (V).

Hence the group delay can be written as:

$$\tau_g = \frac{1}{c}\left[N_{g2} + n_2\Delta\,\frac{d(Vb)}{dV}\right] \tag{2.114}$$

The initial term in Eq. (2.114) gives the dependence of the group delay on wavelength caused when a uniform plane wave is propagating in an infinitely extended medium with a refractive index which is equivalent to that of the fiber cladding. However, the second term results from the waveguiding properties of the fiber only and is determined by the mode delay factor $d(Vb)/dV$, which describes the change in group delay caused by the changes in power distribution between the fiber core and cladding. The mode delay factor [Ref. 50] is a further universal parameter which plays a major part in the theory of single-mode fibers. Its variation with normalized frequency for the fundamental mode in a step index fiber is shown in Figure 2.33.

2.5.5 The Gaussian approximation

The field shape of the fundamental guided mode within a single-mode step index fiber for two values of normalized frequency is displayed in Figure 2.34. As may be expected, considering the discussion in Section 2.4.1, it has the form of a Bessel function ($J_0(r)$) in the core region matched to a modified Bessel function ($K_0(r)$) in the cladding. Depending on the value of the normalized frequency a significant proportion of the modal power is propagated in the cladding region, as mentioned

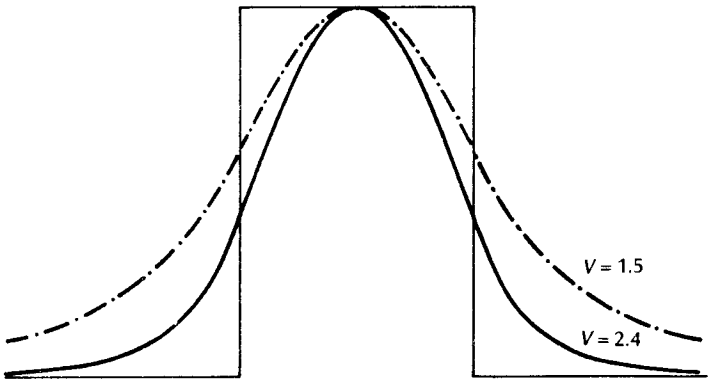

Figure 2.34 Field shape of the fundamental mode for normalized frequencies, $V = 1.5$ and $V = 2.4$.

earlier. Hence, even at the cutoff value (i.e. V_c) only about 80% of the power propagates within the fiber core.

It may be observed from Figure 2.34 that the shape of the fundamental LP_{01} mode is similar to a Gaussian shape, which allows an approximation of the exact field distribution by a Gaussian function.* The approximation may be investigated by writing the scalar wave equation Eq. (2.27) in the form:

$$\nabla^2\psi + n^2k^2\psi = 0 \tag{2.115}$$

where k is the propagation vector defined in Eq. (2.33) and $n(x, y)$ is the refractive index of the fiber, which does not generally depend on z, the coordinate along the fiber axis. It should be noted that the time dependence $\exp(j\omega t)$ has been omitted from the scalar wave equation to give the reduced wave equation† in Eq. (2.115) [Ref. 23]. This representation is valid since the guided modes of a fiber with a small refractive index difference (i.e. $\Delta \ll 1$) have one predominant transverse field component, for example E_y. By contrast E_x and the longitudinal component are very much smaller [Ref. 23].

The field of the fundamental guided mode may therefore be considered as a scalar quantity and need not be described by the full set of Maxwell's equations. Hence Eq. (2.115) may be written as:

$$\nabla^2\phi + n^2k^2\phi = 0 \tag{2.116}$$

where ϕ represents the dominant transverse electric field component.

The near Gaussian shape of the predominant transverse field component of the fundamental mode has been demonstrated [Ref. 51] for fibers with a wide range of refractive index distributions. This proves to be the case not only for the LP_{01}

However, it should be noted that $K_0(r)$ decays as $\exp(-r)$ which is much slower than a true Gaussian.
Eq. (2.115) is also known as the Helmholtz equation.

mode of the step index fiber but also for the modes with fibers displaying arbitrary graded refractive index distributions. Therefore, the predominant electric field component of the single guided mode may be written as the Gaussian function [Ref. 23]:

$$\phi = \left(\frac{2}{\pi}\right)^{\frac{1}{2}} \frac{1}{\omega_0} \exp\left(-r^2/\omega_0^2\right) \exp\left(-j\beta z\right) \tag{2.117}$$

where the radius parameter $r^2 = x^2 + y^2$, ω_0 is a width parameter which is often called the spot size or radius of the fundamental mode (see Section 2.5.2) and β is the propagation constant of the guided mode field.

The factor preceding the exponential function is arbitrary and is chosen for normalization purposes. If it is accepted that Eq. (2.117) is to a good approximation the correct shape [Ref. 26], then the parameters β and ω_0 may be obtained either by substitution [Ref. 52] or by using a variational principle [Ref. 26]. Using the latter tecnnique solutions of the wave equation, Eq. (2.116), are claimed to be functions of the minimum integral:

$$J = \int_V \left[(\nabla\phi)\cdot(\nabla\phi^*) - n^2k^2\phi\,\phi^*\right] \mathrm{d}V = \min \tag{2.118}$$

where the asterisk indicates complex conjugation. The integration range in Eq. (2.118) extends over a large cylinder with the fiber at its axis. Moreover, the length of the cylinder L is arbitrary and its radius is assumed to tend towards infinity.

Use of variational calculus [Ref. 53] indicates that the wave equation Eq. (2.116) is the Euler equation of the variational expression given in Eq. (2.118). Hence, the functions that minimize J satisfy the wave equation. Firstly, it can be shown [Ref. 23] that the minimum value of J is zero if ϕ is a legitimate guided mode field. We do this by performing a partial integration Eq. (2.118) which can be written as:

$$J = \int_s \phi^*(\nabla\phi)\,\mathrm{d}s - \int_V \left[\nabla^2\phi + n^2k^2\phi\right]\phi^*\,\mathrm{d}V \tag{2.119}$$

where the surface element $\mathrm{d}s$ represents a vector in a direction normal to the outside of the cylinder. However, the function ϕ for a guided mode disappears on the curved cylindrical surface with infinite radius. In this case the guided mode field may be expressed as:

$$\phi = \hat{\phi}(x, y) \exp\left(-j\beta z\right) \tag{2.120}$$

It may be observed from Eq. (2.120) that the z dependence is limited to the exponential function and therefore the integrand of the surface integral in Eq. (2.119) is independent of z. This indicates that the contributions to the surface integral from the two end faces of the cylinder are equal in value, opposite in sign and independent of the cylinder length. Thus the entire surface integral goes to zero. Moreover, when the function ϕ is a solution of the wave equation, the volume integral in Eq. (2.119) is zero and hence J is also equal to zero.

The variational expression given in Eq. (2.118) can now be altered by substituting Eq. (2.120). In this case the volume integral becomes an integral over the infinite cross section of the cylinder (i.e. the fiber) which may be integrated over the length coordinate z. Integration over z effectively multiplies the remaining integral over the cross section by the cylinder length L because the integrand is independent of z. Hence dividing by L we can write:

$$\frac{J}{L} = \int_{-\infty}^{\infty} \int_{-\infty}^{\infty} \{(\nabla_t \hat{\phi})(\Delta_t \hat{\phi}^*) - [n^2(x, y)k^2 - \beta^2]\hat{\phi}\hat{\phi}^*\} \, dx \, dy \tag{2.121}$$

where the operator V_t indicates the transverse part (i.e. the x and y derivatives) of Δ.

We have now obtained in Eq. (2.121) the required variational expression that will facilitate the determination of spot size and propagation constant for the guided mode field. The latter parameter may be obtained by solving Eq. (2.121) for β^2 with $J = 0$, as has been proven to be the case for solutions of the wave equation. Thus:

$$\beta^2 = \frac{\int_{-\infty}^{\infty} \int_{-\infty}^{\infty} [n^2 k^2 \hat{\phi}\hat{\phi}^* - (\nabla_t \hat{\phi})(\nabla_t \hat{\phi}^*)] \, dx \, dy}{\int_{-\infty}^{\infty} \int_{-\infty}^{\infty} \hat{\phi}\hat{\phi}^* \, dx \, dy} \tag{2.122}$$

Equation (2.122) allows calculation of the propagation constant of the fundamental mode if the function ϕ is known. However, the integral expression in Eq. (2.122) exhibits a stationary value such that it remains unchanged to the first order when the exact mode function $\hat{\phi}$ is substituted by a slightly perturbed function. Hence a good approximation to the propagation constant can be obtained using a function that only reasonably approximates to the exact function. The Gaussian approximation given in Eq. (2.117) can therefore be substituted into Eq. (2.122) to obtain:

$$\beta^2 = \left[\frac{4k^2}{\omega_0^2} \int_0^{\infty} r n^2(r) \exp(-2r^2/\omega_0^2) \, dr\right] - \frac{2}{\omega_0^2} \tag{2.123}$$

Two points should be noted in relation to Eq. (2.123). Firstly, following Marcuse [Ref. 23] the normalization was picked to bring the denominator of Eq. (2.122) to unity. Secondly, the stationary expression of Eq. (2.123) was obtained from Eq. (2.122) by assuming that the refractive index was dependent only upon the radial coordinate r. This condition is, however, satisfied by most common optical fibre types.

Finally, to derive an expression for the spot size ω_0 we again make use of the stationary property of Eqs. (2.122) and (2.123). Hence, if the Gaussian function of Eq. (2.117) is the correct mode function to give a value for ω_0, then β^2 will not alter if ω_0 is changed slightly. This indicates that the derivative of β^2 with respect to ω_0 becomes zero (i.e. $d\beta^2/d\omega_0 = 0$). Therefore, differentiation of Eq. (2.123) and setting the result to zero yields:

$$1 + 2k^2 \int_0^{\infty} r\left(\frac{2r^2}{\omega_0^2} - 1\right) n^2(r) \exp(-2r^2/\omega_0^2) \, dr = 0 \tag{2.124}$$

Equation (2.124) allows the Gaussian approximation for the fundamental mode within single-mode fiber to be obtained by providing a value for the spot size ω_0. This value may be utilized in Eq. (2.123) to determine the propagation constant β.

For step index profiles it can be shown [Ref. 52] that an optimum value of the spot size ω_0 divided by the core radius is only a function of the normalized frequency V. The optimum values of ω_0/a can be approximated to better than 1% accuracy by the empirical formula [Ref. 52]:

$$\frac{\omega_0}{a} = 0.65 + 1.619\,V^{-\frac{3}{2}} + 2.879\,V^{-6} \tag{2.125}$$

$$= 0.65 + 1.619\left(2.40\,\frac{\lambda_c}{\lambda}\right)^{-\frac{3}{2}} + 2.879\left(2.405\,\frac{\lambda_c}{\lambda}\right)^{-6}$$

$$\omega_0 = a\left[0.65 + 0.434\left(\frac{\lambda}{\lambda_c}\right)^{\frac{3}{2}} + 0.0149\left(\frac{\lambda}{\lambda_c}\right)^{6}\right] \tag{2.126}$$

The approximate expression for spot size given in Eq. (2.126) is frequently used to determine the parameter for step index fibers over the usual range of λ/λ_c (i.e. 0.8 to 1.9) [Ref. 43].

Example 2.10

Estimate the fiber core diameter for a single-mode step index fiber which has a MFD of 11.6 μm when the normalized frequency is 2.2.

Solution: Using the Gaussian approximation, from Eq. (2.125) the fiber core radius is:

$$a = \frac{\omega_0}{0.65 + 1.619(V)^{-\frac{3}{2}} + 2.879(\quad)^{-6}}$$

$$= \frac{5.8 \times 10^{-6}}{0.65 + 1.619(2.2)^{-\frac{3}{2}} + 2.879(2.2)^{-6}}$$

$$= 4.95\ \mu\text{m}$$

Hence the fiber core diameter is 9.9 μm.

The accuracy of the Gaussian approximation has also been demonstrated for graded index fibers [Ref. 54], having a refractive index profile given by Eq. (2.76) (i.e. power law profiles in the core region). When the near parabolic refractive index profile is considered (i.e. $\alpha = 2$) and the square law medium is assumed to extend to infinity rather than to the cladding where $n(r) = n_2$, for $r \geq a$ (Eq. (2.76)); then

the Gaussian spot size given in Eq. (2.124) reduces to:

$$\omega_0^2 = \frac{a}{n_1 k}\left(\frac{2}{\Delta}\right)^{\frac{1}{2}} \tag{2.127}$$

Furthermore, the propagation constant becomes:

$$\beta^2 = n_1^2 k^2\left[1 - \frac{2(2\Delta)^{\frac{1}{2}}}{n_1 k a}\right] \tag{2.128}$$

It is interesting to note that the above relationships for ω_0 and β in this case are identical to the solutions obtained from exact analysis of the square law medium [Ref. 26].

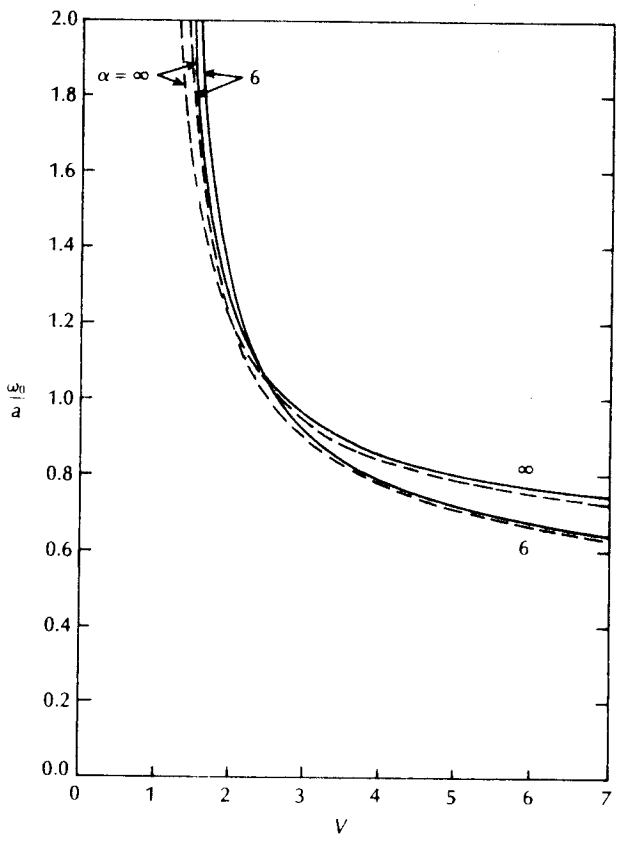

Figure 2.35 Comparison of ω_0/a approximation obtained from Eqs. (2.123) and (2.124) (broken lines) with values obtained from numerical integration of the wave equation and subsequent optimization of its width (solid lines). Reproduced with permission from D. Marcuse, 'Gaussian approximation of the fundamental modes of graded-index fibers', *J. Opt. Soc. Am.*, **68**, p. 103, 1978.

Numerical solutions of Eqs. (2.123) and (2.124) are shown in Figure 2.35 (broken lines) for values of α of 6 and ∞ for profiles with constant refractive indices in the cladding region [Ref. 51]. In this case Eqs. (2.123) and (2.124) cannot be solved analytically and computer solutions must be obtained. The solid lines in Figure 2.35 show the corresponding solutions of the wave equation, also obtained by a direct numerical technique. These results for the spot size and propagation constant are provided for comparison as they are not influenced by the prior assumption of Gaussian shape.

The Gaussian approximation for the transverse field distribution is very much simpler than the exact solution and is very useful for calculations involving both launching efficiency at the single-mode fiber input as well as coupling losses at splices or connectors. In this context it describes very well the field inside the fiber core and provides good approximate values for the guided mode propagation constant. It is a particularly good approximation for fibers operated near the cutoff wavelength of the second order mode [Ref. 26] but when the wavelength increases, the approximation becomes less accurate. In addition, for single-mode fibers with homogeneous cladding, the true field distribution is never exactly Gaussian since the evanescent field in the cladding tends to a more exponential function for which the Gaussian provides an underestimate.

However, for the calculations involving cladding absorption, bend losses, crosstalk between fibers and the properties of directional couplers, then the Gaussian approximation should not be utilized [Ref. 26]. Better approximations for the field profile in these cases can, however, be employed such as the exponential function [Ref. 55], or the modified Hankel function of zero order [Ref. 56], giving the Gaussian-exponential and the Gaussian–Hankel approximations respectively. Unfortunately, these approximations lose the major simplicity of the Gaussian approximation, in which essentially one parameter (the spot size) defines the radial amplitude distribution, because they necessitate two parameters to characterize the same distribution.

2.5.6 Equivalent step index methods

Another strategy to obtain approximate values for the cutoff wavelength and spot size in graded index single-mode fibers (or arbitrary refractive index profile fibers) is to define an equivalent step index (ESI) fiber on which to model the fiber to be investigated. Various methods have been proposed in the literature [e.g. Refs. 57 to 62] which commence from the observation that the fields in the core regions of graded index fibers often appear similar to the fields within step index fibers. Hence, as step index fiber characteristics are well known, it is convenient to replace the exact methods for graded index single-mode fibers [Refs. 63, 64] by approximate techniques based on step index fibers. In addition, such ESI methods allow the propagation characteristics of single-mode fibers to be represented by a few parameters.

Several different suggestions have been advanced for the choice of the core radius a_{ESI}, and the relative index difference Δ_{ESI}, of the ESI fiber which lead to good approximations for the spot size (and hence joint and bend losses) for the actual graded index fiber. They are all conceptually related to the Gaussian approximation (see Section 2.5.5) in that they utilize the close resemblance of the field distribution of the LP_{01} mode to the Gaussian distribution within single-mode fiber. An early proposal for the ESI method [Ref. 58] involved transformation of the basic fiber parameters following:

$$a_s = Xa, \qquad V_s = YV, \qquad NA_s = (Y/X)NA \tag{2.129}$$

where the subscript s is for the ESI fiber and X, Y are constants which must be determined. However, these ESI fiber representations are only valid for a particular value of normalized frequency V and hence there is a different X, Y pair for each wavelength. The transformation can be carried out either on the basis of compared radii or relative refractive index differences. Figure 2.36 compares the refractive index profiles and the electric field distributions for two graded index fibres ($\alpha = 2, 4$) and their ESI fibers. It may be observed that their fields differ slightly only near the axis.

An alternative ESI technique is to normalize the spot size ω_0 with respect to an optimum effective fiber core radius a_{eff} [Ref. 61]. This latter quantity is obtained from the experimental measurement of the first minimum (angle θ_{min}) in the diffraction pattern using transverse illumination of the fiber immersed in an index matching fluid. Hence:

$$a_{eff} = 3.832/k \sin \theta_{min} \tag{2.130}$$

where $k = 2\pi/\lambda$. In order to obtain the full comparison with single-mode step index fiber, the results may be expressed in terms of an effective normalized frequency V_{eff} which relates the cutoff frequencies/wavelengths for the two fibers:

$$V_{eff} = 2.405(V/V_c) = 2.405(\lambda_c/\lambda) \tag{2.131}$$

The technique provides a dependence of ω_0/a_{eff} on V_{eff} which is almost identical for a reasonably wide range of profiles which are of interest for minimizing dispersion (i.e. $1.5 < V_{eff} < 2.4$).

A good analytical approximation for this dependence is given by [Ref. 61]:

$$\frac{\omega_0}{a_{eff}} = 0.6043 + 1.755\, V_{eff}^{-\frac{3}{2}} + 2.78\, V_{eff}^{-6} \tag{2.132}$$

Refractive index profile dependent deviations from the relationship shown in Eq. (2.132) are within $\pm 2\%$ for general power law graded index profiles.

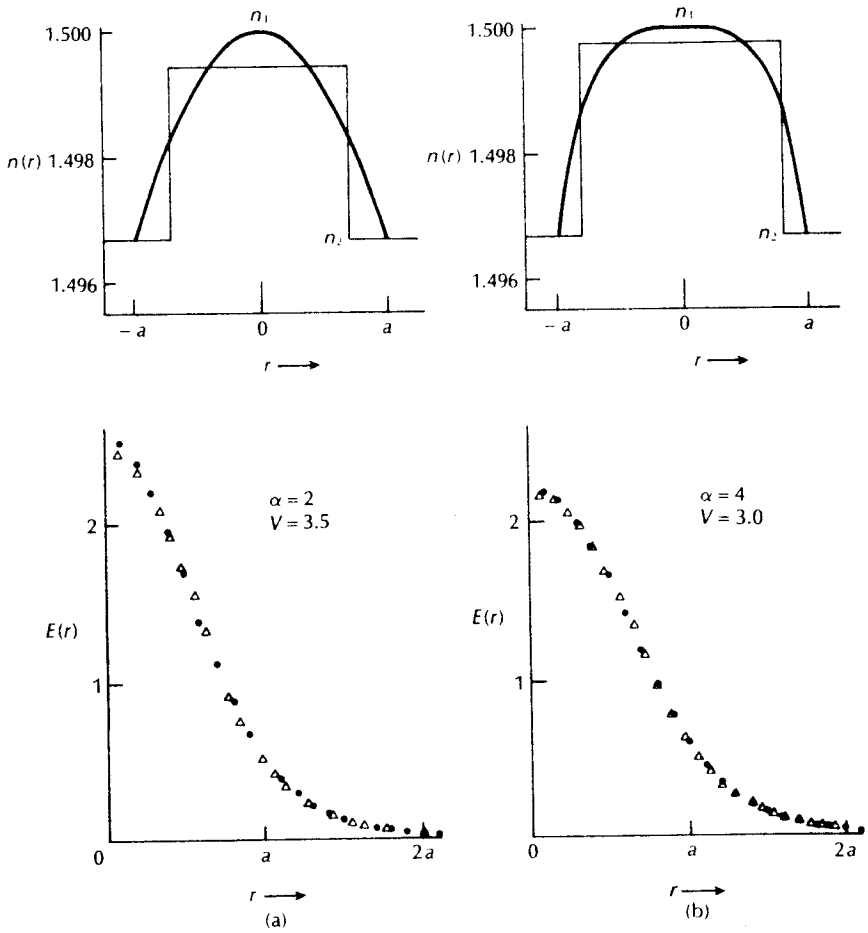

Figure 2.36 Refractive index distributions $n(r)$ and electric field distributions $E(r)$ for graded index fibers and their ESI fibers for: (a) $\alpha = 2$, $V = 3.5$; (b) $\alpha = 4$, $V = 3.0$. The field distributions for the graded index and corresponding ESI profiles are shown by solid circles and open triangles respectively. Reproduced with permission from H. Matsumura and T. Suganuma, *Appl. Opt.*, **19**, p. 3151, 1980.

Example 2.11

A parabolic profile graded index single-mode fiber designed for operation at a wavelength of 1.30 μm has a cutoff wavelength of 1.08 μm. From experimental measurement it is established that the first minimum in the diffraction pattern occurs at an angle of 12°. Using an ESI technique, determine the spot size at the operating wavelength.

Solution: Using Eq. (2.130), the effective core radius is:

$$a_{\text{eff}} = \frac{3.832\lambda}{2\pi \sin \theta_{\min}} = \frac{3.832 \times 1.30 \times 10^{-6}}{2\pi \sin 12^{\circ}}$$

$$= 3.81\ \mu\text{m}$$

The effective normalized frequency can be obtained from Eq. (2.131) as:

$$V_{\text{eff}} = 2.405 \frac{\lambda_c}{\lambda} = 2.405 \frac{1.08}{1.30} = 2.00$$

Hence the spot size is given by Eq. (2.132) as:

$$\omega_0 = 3.81 \times 10^{-6}[0.6043 + 1.755(2.00)^{-\frac{3}{2}} + 2.78(2.00)^{-6}]$$
$$= 4.83\ \mu\text{m}$$

Other ESI methods involve the determination of the equivalent parameters from experimental curves of spot size against wavelength [Ref. 62]. All require an empirical formula, relating spot size to the normalized frequency for a step index fiber, to be fitted by some means to the data. The usual empirical formula employed is that derived by Marcuse for the Gaussian approximation and given in Eq. (2.125). An alternative formula which is close to Eq. (2.125) is provided by Snyder [Ref. 65] as:

$$\omega_0 = a(\ln V)^{-\frac{1}{2}} \tag{2.133}$$

However, it is suggested [Ref. 62] that the expression given in Eq. (2.133) is probably less accurate than that provided by Eq. (2.125).

A cutoff method can also be utilized to obtain the ESI parameters [Ref. 66]. In this case the cutoff wavelength λ_c and spot size ω_0 are known. Therefore, substituting $V = 2.405$ into Eq. (2.125) gives:

$$\omega_0 = 1.099 a_{\text{ESI}} \text{ or } 2a_{\text{ESI}} = 1.820\omega_0 \tag{2.134}$$

Then using Eq. (2.70) the ESI relative index difference is:

$$\Delta_{\text{ESI}} = (0.293/n_1^2)(\lambda_c/2a_{\text{ESI}})^2 \tag{2.135}$$

where n_1 is the maximum refractive index of the fiber core.

Example 2.12

Obtain the ESI relative refractive index difference for a graded index fiber which has a cutoff wavelength and spot size of 1.190 μm and 5.2 μm respectively. The maximum refractive index of the fiber core is 1.485.

Solution: The ESI core radius may be obtained from Eq. (2.134) where:

$$2a_{ESI} = 1.820 \times 5.2 \times 10^{-6} = 9.464\ \mu m$$

Using Eq. (2.135), the ESI relative index difference is given by:

$$\Delta_{ESI} = (0.293/1.485^2)(1.190/9.464)^2$$
$$= 2.101 \times 10^{-3} \text{ or } 0.21\%$$

Alternatively, performing a least squares fit on Eq. (2.125) provides 'best values' for the ESI diameter ($2a_{ESI}$) and relative index difference (Δ_{ESI}) [Ref. 62]. It must be noted, however, that these best values are dependent on the application and the least squares method appears most useful in estimating losses at fiber joints [Ref. 67]. In addition, recent work [Ref. 68] has attempted to provide a more consistent relationship between the ESI parameters and the fiber mode-field diameter. Overall, the concept of the ESI fiber has been relatively useful in the specification of standard matched-cladding and depressed-cladding fibers by their equivalent a_{ESI} and Δ_{ESI} values. Unfortunately, ESI methods are unable accurately to predict mode-field diameters and waveguide dispersion in dispersion shifted and dispersion flattened (see Section 3.12) fibers [Ref. 19].

Problems

2.1 Using simple ray theory, describe the mechanism for the transmission of light within an optical fiber. Briefly discuss with the aid of a suitable diagram what is meant by the acceptance angle for an optical fiber. Show how this is related to the fiber numerical aperture and the refractive indices for the fiber core and cladding.

An optical fiber has a numerical aperture of 0.20 and a cladding refractive index of 1.59. Determine:

(a) the acceptance angle for the fiber in water which has a refractive index of 1.33;
(b) the critical angle at the core–cladding interface.

Comment on any assumptions made about the fiber.

2.2 The velocity of light in the core of a step index fiber is $2.01 \times 10^8\ m\,s^{-1}$, and the critical angle at the core–cladding interface is 80°. Determine the numerical aperture and the acceptance angle for the fiber in air, assuming it has a core diameter suitable for consideration by ray analysis. The velocity of light in a vacuum is $2.998 \times 10^3\ m\,s^{-1}$

2.3 Define the relative refractive index difference for an optical fiber and show how it may be related to the numerical aperture.

A step index fiber with a large core diameter compared with the wavelength of the transmitted light has an acceptance angle in air of 22° and a relative refractive index difference of 3%. Estimate the numerical aperture and the critical angle at the core–cladding interface for the fiber.

2.4 A step index fiber has a solid acceptance angle in air of 0.115 radians and a relative refractive index difference of 0.9%. Estimate the speed of light in the fiber core.

2.5 Briefly indicate with the aid of suitable diagrams the difference between meridional and skew ray paths in step index fibers.

Derive an expression for the acceptance angle for a skew ray which changes direction by an angle 2γ at each reflection in a step index fiber in terms of the fiber NA and γ. It may be assumed that ray theory holds for the fiber.

A step index fiber with a suitably large core diameter for ray theory considerations has core and cladding refractive indices of 1.44 and 1.42 respectively. Calculate the acceptance angle in air for skew rays which change direction by 150° at each reflection.

2.6 Skew rays are accepted into a large core diameter (compared to the wavelength of the transmitted light) step index fiber in air at a maximum axial angle of 42°. Within the fiber they change direction by 90° at each reflection. Determine the acceptance angle for meridional rays for the fiber in air.

2.7 Explain the concept of electromagnetic modes in relation to a planar optical waveguide.

Discuss the modifications that may be made to electromagnetic mode theory in a planar waveguide in order to describe optical propagation in a cylindrical fiber.

2.8 Briefly discuss, with the aid of suitable diagrams, the following concepts in optical fiber transmission:

(a) the evanescent field;
(b) Goos–Haenchen shift;
(c) mode coupling.

Describe the effects of these phenomena on the propagation of light in optical fibers.

2.9 Define the normalized frequency for an optical fiber and explain its use in the determination of the number of guided modes propagating within a step index fiber.

A step index fiber in air has a numerical aperture of 0.16, a core refractive index of 1.45 and a core diameter of 60 μm. Determine the normalized frequency for the fiber when light at a wavelength of 0.9 μm is transmitted. Further, estimate the number of guided modes propagating in the fiber.

2.10 Describe with the aid of simple ray diagrams:

(a) the multimode step index fiber;
(b) the single-mode step index fiber.

Compare the advantages and disadvantages of these two types of fiber for use as an optical channel.

2.11 A multimode step index fiber has a relative refractive index difference of 1% and a core refractive index of 1.5. The number of modes propagating at a wavelength of 1.3 μm is 1100. Estimate the diameter of the fiber core.

2.12 Explain what is meant by a graded index optical fiber, giving an expression for the possible refractive index profile. Using simple ray theory concepts, discuss the transmission of light through the fiber. Indicate the major advantage of this type of fiber with regard to multimode propagation.

2.13 The relative refractive index difference between the core axis and the cladding of a graded index fiber is 0.7% when the refractive index at the core axis is 1.45. Estimate values for the numerical aperture of the fiber when:

(a) the index profile is not taken into account; and
(b) the index profile is assumed to be triangular.

Comment on the results.

2.14 A multimode graded index fiber has an acceptance angle in air of 8°. Estimate the

relative refractive index difference between the core axis and the cladding when the refractive index at the core axis is 1.52.

2.15 The WKB value for the propagation constant β given in Eq. (2.91) in a parabolic refractive index core fiber assumes an infinitely extended parabolic profile medium. When in a practical fiber the parabolic index profile is truncated, show that the mode numbers m and l are limited by the following condition:

$$2(2m + l + 1) \leqslant ka(n_1^2 - n_2^2)^{\frac{1}{2}}$$

2.16 A graded index fiber with a parabolic index profile supports the propagation of 742 guided modes. The fiber has a numerical aperture in air of 0.3 and a core diameter of 70 μm. Determine the wavelength of the light propagating in the fiber.

Further estimate the maximum diameter of the fiber which gives single-mode operation at the same wavelength.

2.17 A graded index fiber with a core axis refractive index of 1.5 has a characteristic index profile (α) of 1.90, a relative refractive index difference of 1.3% and a core diameter of 40 μm. Estimate the number of guided modes propagating in the fiber when the transmitted light has a wavelength of 1.55 μm, and determine the cutoff value of the normalized frequency for single-mode transmission in the fiber.

2.18 A single-mode step index fiber has a core diameter of 7 μm and a core refractive index of 1.49. Estimate the shortest wavelength of light which allows single-mode operation when the relative refractive index difference for the fiber is 1%.

2.19 In problem 2.18, it is required to increase the fiber core diameter to 10 μm whilst maintaining single-mode operation at the same wavelength. Estimate the maximum possible relative refractive index difference for the fiber.

2.20 Show that the maximum value of a/λ is approximately 1.4 times larger for a parabolic refractive index profile single-mode fiber than for a single-mode step index fiber. Hence, sketch the relationship between the maximum core diameter and the propagating optical wavelength which will facilitate single-mode transmission in the parabolic profile fiber.

2.21 A single-mode step index fiber which is designed for operation at a wavelength of 1.3 μm has core and cladding refractive indices of 1.447 and 1.442 respectively. When the core diameter is 7.2 μm, confirm that the fiber will permit single-mode transmission and estimate the range of wavelengths over which this will occur.

2.22 A single-mode step index fiber has core and cladding refractive indices of 1.498 and 1.495 respectively. Determine the core diameter required for the fiber to permit its operation over the wavelength range 1.48 to 1.60 μm. Calculate the new fiber core diameter to enable single-mode transmission at a wavelength of 1.30 μm.

2.23 A single-mode fiber has a core refractive index of 1.47. Sketch a design characteristic of relative refractive index difference Δ against core radius for the fiber to operate at a wavelength of 1.30 μm. Determine whether the fiber remains single-mode at a transmission wavelength of 0.85 μm when its core radius is 4.5 μm.

2.24 Convert the approximation for the normalized propagation constant of a single-mode step index fiber given in Example 2.9 into a relationship involving the normalized wavelength λ/λ_c in place of the normalized frequency. Hence, determine the range of values of this parameter over which the relative error in the approximation is between 0.2% and 2%.

2.25 Given that the Gaussian function for the electric field distribution of the fundamental mode in a single-mode fiber of Eq. (2.117) takes the form:

$$\Gamma(r) = E_0 \exp(-r^2/\omega_0^2)$$

where $E(r)$ and E_0 are shown in Figure 2.31, use the approximation of Eq. (2.125) to evaluate and sketch $E(r)/E_0$ against r/a over the range 0 to 3 for values of normalized frequency $V = 1.0, 1.5, 2.0, 2.5, 3.0$.

2.26 The approximate expression provided in Eq. (2.125) is valid over the range of normalized frequency $1.2 < V < 2.4$. Sketch ω_0/a against V over this range for the fundamental mode in a step index fiber. Comment on the magnitude of ω_0/a as the normalized frequency is reduced significantly below 2.4 and suggest what this indicates about the distribution of the light within the fiber.

2.27 The spot size in a parabolic profile graded index single-mode fiber is 11.0 μm at a transmission wavelength of 1.55 μm. In addition, the cutoff wavelength for the fiber is 1.22 μm. Using an ESI technique, determine the fiber effective core radius and hence estimate the angle at which the first minimum in the diffraction pattern from the fiber would occur.

2.28 The cutoff method is employed to obtain the ESI parameters for a graded index single-mode fiber. If the ESI relative index difference was found to be 0.30% when the spot size and cutoff wavelength were 4.6 μm and 1.29 μm, respectively, calculate the maximum refractive index of the fiber core.

Answers to numerical problems

2.1 (a) 8.6°; (b) 83.6°
2.2 0.263, 15.2°
2.3 0.375, 75.9°
2.4 2.11×10^8 m s^{-1}
2.5 34.6°
2.6 28.2°
2.9 33.5, 561
2.11 92 μm
2.13 (a) 0.172; (b) 0.171
2.14 0.42%
2.16 1.2 μm, 4.4 μm
2.17 94, 3.45
2.18 1.36 μm
2.19 0.24%
2.21 down to 1139 nm
2.22 12.0 μm, 10.5 μm
2.24 $0.8 \leqslant \lambda/\lambda_c \leqslant 1.0$ and $1.6 \leqslant \lambda/\lambda_c \leqslant 2.4$
2.27 3.0 μm, 18.4°
2.28 1.523

References

[1] D. Hondros and P. Debye, 'Electromagnetic waves along long cylinders of dielectric', *Annal. Physik*, **32**(3), pp. 465–476, 1910.
[2] O. Schriever, 'Electromagnetic waves in dielectric wires', *Annal. Physik*, **63**(7), pp. 645–673, 1920.
[3] A. C. S. van Heel, 'A new method of transporting optical images without aberrations', *Nature, Lond.*, **173**, p. 39, 1954.
[4] H. H. Hopkins and N. S. Kapany, 'A flexible fibrescope, using static scanning', *Nature, Lond.*, **113**, pp. 39–41, 1954.
[5] K. C. Kao and G. A. Hockham, 'Dielectric-fibre surface waveguides for optical frequencies', *Proc IEE*, **113**, pp. 1151–1158, 1966.
[6] A. Werts, 'Propagation de la lumière coherente dans les fibres optiques', *L'Onde Electrique*, **46**, pp. 967–980, 1966.
[7] S. Takahashi and T. Kawashima, 'Preparation of low loss multi-component glass fiber', *Tech. Dig. Int. Conf. Integr. Opt. and Opt. Fiber Commun.*, p. 621, 1977.

[8] J. B. MacChesney, P. B. O'Connor, F. W. DiMarcello, J. R. Simpson and P. D. Lazay, 'Preparation of low-loss optical fibres using simultaneous vapour phase deposition and fusion', *Proc. 10th Int. Conf. on Glass*, paper 6–40, 1974.
[9] T. Miya, Y. Terunuma, T. Hosaka and T. Miyashita, 'Ultimate low-loss single-mode fibre at 1.55 μm', *Electron Lett.*, **15**(4), pp. 106–108, 1979.
[10] S. Sakaguchi, 'Low loss optical fibers for midinfrared optical communication', *J. of Lightwave Technol.*, **LT-5**(9), pp. 1219–1228, 1987.
[11] M. Born and E. Wolf, *Principles of Optics*, 6th edn., Pergamon Press, 1980.
[12] D. C. Agarwal, 'Ray concepts in optical fibers', *Indian J. Theoret. Phys.*, **28**(1), pp. 41–54, 1980.
[13] R. P. Feyman, *The Feyman Lectures on Physics*, Vol. 2, Addison-Wesley, 1969.
[14] J. E. Midwinter, *Optical Fibers for Transmission*, John Wiley, 1979.
[15] E. Snitzer, 'Cylindrical dielectric waveguide modes', *J. Opt. Soc. Am.*, **51**, pp. 491–498, 1961.
[16] D. Gloge, 'Weakly guiding fibers', *Appl. Opt.*, **10**, pp. 2252–2258, 1971.
[17] D. Marcuse, *Theory of Dielectric Optical Waveguides*, Academic Press, New York, 1974.
[18] A. W. Snyder, 'Asymptotic expressions for eigenfunctions and eigenvalues of a dielectric or optical waveguide', *Trans IEEE Microwave Theory Tech.*, **MTT-17**, pp. 1130–1138, 1969.
[19] E. G. Neumann, *Single-Mode Fibers: Fundamentals*, Springer-Verlag, 1988.
[20] D. Gloge, 'Optical power flow in multimode fibers', *Bell Syst. Tech. J.*, **51**, pp. 1767–1783, 1972.
[21] R. Olshansky, 'Propagation in glass optical waveguides', *Rev. Mod. Phys.*, **51**(2), pp. 341–366, 1979.
[22] P. M. Morse and H. Fesbach, *Methods of Theoretical Physics*, Vol. II, McGraw-Hill, 1953.
[23] D. Marcuse, *Light Transmission Optics*, 2nd edn, Van Nostrand Reinhold, 1982.
[24] A. Ghatak and K. Thyagarajan, 'Graded index optical waveguides', in E. Wolf (ed.), *Progress in Optics Vol. XVIII*, pp. 3–128, North-Holland 1980.
[25] D. B. Beck, 'Optical fiber waveguides', in M. K. Barnoski (Ed.), *Fundamentals of Optical Fiber Communications*, pp. 1–58, Academic Press, 1976.
[26] D. Marcuse, D. Gloge, E. A. J. Marcatili, 'Guiding properties of fibers', in *Optical Fiber Telecommunications*, S. E. Miller and A. G. Chynoweth (Eds.), Academic Press, pp. 37–100, 1979.
[27] I. S. Gradshteyn and I. M. Ryzhik, *Tables of Integrals, Series and Products*, 4th edn, Academic Press, 1965.
[28] K. Okamoto and T. Okoshi, 'Analysis of wave propagation in optical fibers having core with α-power refractive-index distribution and uniform cladding', *IEEE Trans. Microwave Theory Tech.*, **MTT-24**, pp. 416–421, 1976.
[29] M. A. Saifi, 'Triangular index monomode fibres' in *Proc. SPIE Int. Soc. Opt. Eng. (USA)*, **374**, pp. 13–15, 1983.
[30] D. Gloge, 'The optical fibre as a transmission medium', *Rep. Prog. Phys.*, **42**, pp. 1777–1824, 1979.
[31] M. M. Ramsey and G. A. Hockham, 'Propagation in optical fibre waveguides' in C. P. Sandbank (Ed.) *Optical Fibre Communication Systems*, pp. 25–41, John Wiley, 1980.

[32] S. Kawakami and S. Nishida, 'Characteristics of a doubly clad optical fiber with a low index cladding', *IEEE J. Quantum Electron*, **QE-10**, pp. 879–887, 1974.
[33] C. W. Yeh, 'Optical waveguide theory', *IEEE Trans. Circuits and Syst.*, **CAS-26**(12), pp. 1011–1019, 1979.
[34] C. Pask and R. A. Sammut, 'Developments in the theory of fibre optics', *Proc. IREE Aust.*, **40**(3), pp. 89–101, 1979.
[35] W. A. Gambling, A. H. Hartog and C. M. Ragdale, 'Optical fibre transmission lines', *The Radio Electron. Eng.*, **51**(7/8), pp. 313–325, 1981.
[36] H. G. Unger, *Planar Optical Waveguides and Fibres*, Clarendon Press, 1977.
[37] M. J. Adams, *An Introduction to Optical Waveguides*, John Wiley, 1981.
[38] Y. Suematsu and K.-I. Iga, *Introduction to Optical Fibre Communications*, John Wiley, 1982.
[39] T. Okoshi, *Optical Fibers*, Academic Press, 1982.
[40] H. Kanamori, H. Yokota, G. Tanaka, M. Watanabe, Y. Ishiguro, I. Yoshida, T. Kakii, S. Itoh, Y. Asano and S. Takana, 'Transmission characteristics and reliability of silica-core single-mode fibers', *J. of Lightwave Technol.*, **LT-4**(8), pp. 1144–1150, 1986.
[41] V. A. Bhagavatula, J. C. Lapp, A. J. Morrow and J. E. Ritter, 'Segmented-core fiber for long-haul and local-area-network applications', *J. of Lightwave Technol.*, **6**(10), pp. 1466–1469, 1988.
[42] D. P. Jablonowski, 'Fiber manufacture at AT&T with the MCVD Process', *J. of Lightwave Technol.*, **LT-4**(8), pp. 1016–1019, 1986.
[43] L. B. Jeunhomme, *Single-Mode Fiber Optics*, Marcel Dekker Inc., 1983.
[44] CCITT, COM XV-83-E, USA, 'Cut-off wavelength of cabled single-mode fibers', 1985.
[45] K. I. White, 'Methods of measurements of optical fiber properties', *J. Phys. E. Sci. Instrum.*, **18**, pp. 813–821, 1985.
[46] K. Petermann, 'Constraints for the fundamental-mode spot size for broadband dispersion-compensated single-mode fibres', *Electron. Lett.*, **19**, pp. 712–714, 1983.
[47] W. T. Anderson, V. Shah, L. Curtis, A. J. Johnson and J. P. Kilmer, 'Mode-Field diameter measurements for single-mode fibers with non-Gaussian field profiles', *J. of Lightwave Technol.*, **LT-5**, pp. 211–217, 1987.
[48] H. Kogelnik and H. P. Weber, 'Rays, stored energy, and power flow in dielectric waveguides', *J. Opt. Soc. Am.*, **64**, pp. 174–185, 1974.
[49] A. W. Snyder and J. D. Love, *Optical Waveguide Theory*, Chapman and Hall, 1983.
[50] H. G. Unger, *Planar Optical Waveguides and Fibres*, Clarendon Press, Oxford, 1977.
[51] D. Marcuse, 'Gaussian approximation of the fundamental modes of graded-index fibers', *J. Opt. Soc. Am.*, **68**(1), pp. 103–109, 1978.
[52] D. Marcuse, 'Loss analysis of single-mode fiber splices', *Bell Syst. Tech. J.*, **56**(5), pp. 703–718, 1977.
[53] G. A. Bliss, *Lectures on the Calculus of Variations*, University of Chicago Press, Chicago, 1946.
[54] D. Marcuse, 'Excitation of the dominant mode of a round fiber by a Gaussian beam', *Bell. Syst. Tech. J.*, **49**, pp. 1695–1703, 1970.
[55] A. K. Ghatak, R. Srivastava, I. F. Faria, K. Thyagaranjan and R. Tiwari, 'Accurate method for characterizing single-mode fibers: theory and experiment', *Electron. Lett.*, **19**, pp. 97–99, 1983.
[56] E. K. Sharma and R. Tewari, 'Accurate estimation of single-mode fiber characteristics from near-field measurements', *Electron. Lett.*, **20**, pp. 805–806, 1984.

[57] A. W. Snyder and R. A. Sammut, 'Fundamental (HE) modes of graded optical fibers', *J. Opt. Soc. Am.*, **69**, pp. 1663–1671, 1979.

[58] H. Matsumura and T. Suganama, 'Normalization of single-mode fibers having arbitrary index profile', *Appl. Opt.*, **19**, pp. 3151–3158, 1980.

[59] R. A. Sammut and A. W. Snyder, 'Graded monomode fibres and planar waveguides', *Electron. Lett.*, **16**, pp. 32–34, 1980.

[60] C. Pask and R. A. Sammut, 'Experimental characterisation of graded-index single-mode fibres', *Electron. Lett.*, **16**, pp. 310–311, 1980.

[61] J. Streckert and E. Brinkmeyer, 'Characteristic parameters of monomode fibers', *Appl. Opt.*, **21**, pp. 1910–1915, 1982.

[62] M. Fox, 'Calculation of equivalent step-index parameters for single-mode fibres', *Opt. and Quantum Electron.*, **15**, pp. 451–455, 1983.

[63] W. A. Gambling and H. Matsumura, 'Propagation in radially-inhomogeneous single-mode fibre', *Opt. and Quantum Electron.*, **10**, pp. 31–40, 1978.

[64] W. A. Gambling, H. Matsumura and C. M. Ragdale, 'Wave propagation in a single-mode fibre with dip in the refractive index', *Opt. and Quantum Electron.*, **10**, pp. 301–309, 1978.

[65] A. W. Snyder, 'Understanding monomode optical fibers', *Proc. IEEE*, **69(1)**, pp. 6–13, 1981.

[66] V. A. Bhagavatula, 'Estimation of single-mode waveguide dispersion using an equivalent-step-index approach', *Electron, Lett.*, **18(8)**, pp. 319–320, 1982.

[67] D. Davidson, 'Single-mode wave propagation in cylindrical optical fibers', *Optical-Fiber Transmission*, E. E. Basch (Ed.), H. W. Sams & Co., pp. 27–64, 1987.

[68] F. Martinez and C. D. Hussey, '(E) ESI determination from mode-field diameter and refractive index profile measurements on single-mode fibers', *IEE Proc. Pt. J.*, **135(3)**, pp. 202–210, 1988.

3

Transmission characteristics of optical fibers

3.1 Introduction

The basic transmission mechanisms of the various types of optical fiber waveguide have been discussed in Chapter 2. However, the factors which affect the performance of optical fibers as a transmission medium were not dealt with in

detail. These transmission characteristics are of utmost importance when the suitability of optical fibers for communication purposes is investigated. The transmission characteristics of most interest are those of attenuation (or loss) and bandwidth.

The huge potential bandwidth of optical communications helped stimulate the birth of the idea that a dielectric waveguide made of glass could be used to carry wideband telecommunication signals. This occurred, as indicated in Section 2.1 in the celebrated papers by Kao and Hockham, and Werts, in 1966. However, at the time the idea may have seemed somewhat ludicrous as a typical block of glass could support optical transmission for at best a few tens of metres before it was attenuated to an unacceptable level. Nevertheless, careful investigation of the attenuation showed that it was largely due to absorption in the glass, caused by impurities such as iron, copper, manganese and other transition metals which occur in the third row of the periodic table. Hence, research was stimulated towards a new generation of 'pure' glasses for use in optical fiber communications.

A major breakthrough came in 1970 when the first fiber with an attenuation below 20 $dB\,km^{-1}$ was reported [Ref. 1]. This level of attenuation was seen as the absolute minimum that had to be achieved before an optical fiber system could in any way compete economically with existing communication systems. Since 1970 tremendous improvements have been made, leading to silica-based glass fibers with losses of less than 0.2 $dB\,km^{-1}$ in the laboratory [Ref. 2]. Hence, comparatively low loss fibers have been incorporated into optical communication systems throughout the world. Moreover, as the fundamental lower limits for attenuation in silicate glass fibers have virtually been achieved, activities are increasing in relation to the investigation of other material systems which may exhibit substantially lower losses when operated at longer wavelengths. Such mid-infrared (and possibly far-infrared) transmitting fibers could eventually provide for extremely long-haul repeaterless communication assuming that, in addition to the material considerations, the optical source and detector requirements can be satisfactorily met [Ref. 2].

The other characteristic of primary importance is the bandwidth of the fiber. This is limited by the signal dispersion within the fiber, which determines the number of bits of information transmitted in a given time period. Therefore, once the attenuation was reduced to acceptable levels attention was directed towards the dispersive properties of fibers. Again, this has led to substantial improvements, giving wideband fiber bandwidths of many tens of gigahertz over a number of kilometres.

In order to appreciate these advances and possible future developments, the optical transmission characteristics of fibers must be considered in greater depth. Therefore, in this chapter we discuss the mechanisms within optical fibers which give rise to the major transmission characteristics mentioned previously (attenuation and dispersion), whilst also considering other, perhaps less obvious, effects when light is propagating down an optical fiber (modal noise, polarization and nonlinear phenomena).

We begin the discussion of attenuation in Section 3.2 with calculation of the total losses incurred in optical fibers. The various attenuation mechanisms (material absorption, linear scattering, nonlinear scattering, fiber bends) are then considered in detail in Sections 3.3 to 3.6. The primary focus within these sections is on silica-based glass fibers. However, in Section 3.7 consideration is given to other material systems which may be employed for mid-infrared and far-infrared optical transmission. Dispersion in optical fibers is described in Section 3.8, together with the associated limitations on fiber bandwidth. Sections 3.9 and 3.10 deal with intramodal and intermodal dispersion mechanisms and included in the latter section is a discussion of the modal noise phenomenon associated with intermodal dispersion. Overall signal dispersion in both multimode and single-mode fibers is then considered in Section 3.11. This is followed in Section 3.12 by discussion of the modification of the dispersion characteristics within single-mode fibers in order to obtain dispersion shifted and dispersion flattened fibers. Section 3.13 presents a brief account of polarization within single-mode fibers which includes description of the salient features of polarization maintaining fibers.

Finally, nonlinear optical phenomena, which can occur at relatively high optical power levels within single-mode fibers, are dealt with in Section 3.14.

3.2 Attenuation

The attenuation or transmission loss of optical fibers has proved to be one of the most important factors in bringing about their wide acceptance in telecommunications. As channel attenuation largely determined the maximum transmission distance prior to signal restoration, optical fiber communications became especially attractive when the transmission losses of fibers were reduced below those of the competing metallic conductors (less than 5 dB km^{-1}).

Signal attenuation within optical fibers, as with metallic conductors, is usually expressed in the logarithmic unit of the decibel. The decibel, which is used for comparing two power levels, may be defined for a particular optical wavelength as the ratio of the input (transmitted) optical power P_i into a fiber to the output (received) optical power P_o from the fiber as:

$$\textit{Number of decibels}\ (\text{dB}) = 10 \log_{10} \frac{P_i}{P_o} \tag{3.1}$$

This logarithmic unit has the advantage that the operations of multiplication and division reduce to addition and subtraction, whilst powers and roots reduce to multiplication and division. However, addition and subtraction require a conversion to numerical values which may be obtained using the relationship:

$$\frac{P_i}{P_o} = 10^{(\text{dB}/10)} \tag{3.2}$$

In optical fiber communications the attenuation is usually expressed in decibels

per unit length (i.e. $dB\,km^{-1}$) following:

$$\alpha_{dB} L = 10 \log_{10} \frac{P_i}{P_o} \tag{3.3}$$

where α_{dB} is the signal attenuation per unit length in decibels and L is the fiber length

---

Example 3.1

When the mean optical power launched into an 8 km length of fiber is 120 μW, the mean optical power at the fiber output is 3 μW.

Determine:

(a) the overall signal attenuation or loss in decibels through the fiber assuming there are no connectors or splices;
(b) the signal attenuation per kilometre for the fiber.
(c) the overall signal attenuation for a 10 km optical link using the same fiber with splices at 1 km intervals, each giving an attenuation of 1 dB;
(d) the numerical input/output power ratio in (c).

Solution: (a) Using Eq. (3.1), the overall signal attenuation in decibels through the fiber is:

$$\textit{Signal attenuation} = 10 \log_{10} \frac{P_i}{P_o} = 10 \log_{10} \frac{120 \times 10^{-6}}{3 \times 10^{-6}}$$

$$= 10 \log_{10} 40 = 16.0 \text{ dB}$$

(b) The signal attenuation per kilometre for the fiber may be simply obtained by dividing the result in (a) by the fiber length which corresponds to it using Eq. (3.3) where,

$$\alpha_{dB} L = 16.0 \text{ dB}$$

hence,

$$\alpha_{dB} = \frac{16.0}{8}$$

$$= 2.0 \text{ dB km}^{-1}$$

(c) As $\alpha_{dB} = 2\ dB\,km^{-1}$, the loss incurred along 10 km of the fiber is given by

$$\alpha_{dB} L = 2 \times 10 = 20 \text{ dB}$$

However, the link also has nine splices (at 1 km intervals) each with an attenuation of 1 dB. Therefore, the loss due to the splices is 9 dB.

optical fibers. The various attenuation mechanisms (material absorption, linear scattering, nonlinear scattering, fiber bends) are then considered in detail in Sections 3.3 to 3.6. The primary focus within these sections is on silica-based glass fibers. However, in Section 3.7 consideration is given to other material systems which may be employed for mid-infrared and far-infrared optical transmission. Dispersion in optical fibers is described in Section 3.8, together with the associated limitations on fiber bandwidth. Sections 3.9 and 3.10 deal with intramodal and intermodal dispersion mechanisms and included in the latter section is a discussion of the modal noise phenomenon associated with intermodal dispersion. Overall signal dispersion in both multimode and single-mode fibers is then considered in Section 3.11. This is followed in Section 3.12 by discussion of the modification of the dispersion characteristics within single-mode fibers in order to obtain dispersion shifted and dispersion flattened fibers. Section 3.13 presents a brief account of polarization within single-mode fibers which includes description of the salient features of polarization maintaining fibers.

Finally, nonlinear optical phenomena, which can occur at relatively high optical power levels within single-mode fibers, are dealt with in Section 3.14.

3.2 Attenuation

The attenuation or transmission loss of optical fibers has proved to be one of the most important factors in bringing about their wide acceptance in telecommunications. As channel attenuation largely determined the maximum transmission distance prior to signal restoration, optical fiber communications became especially attractive when the transmission losses of fibers were reduced below those of the competing metallic conductors (less than 5 dB km^{-1}).

Signal attenuation within optical fibers, as with metallic conductors, is usually expressed in the logarithmic unit of the decibel. The decibel, which is used for comparing two power levels, may be defined for a particular optical wavelength as the ratio of the input (transmitted) optical power P_i into a fiber to the output (received) optical power P_o from the fiber as:

$$\textit{Number of decibels}\ (\text{dB}) = 10 \log_{10} \frac{P_i}{P_o} \tag{3.1}$$

This logarithmic unit has the advantage that the operations of multiplication and division reduce to addition and subtraction, whilst powers and roots reduce to multiplication and division. However, addition and subtraction require a conversion to numerical values which may be obtained using the relationship:

$$\frac{P_i}{P_o} = 10^{(\text{dB}/10)} \tag{3.2}$$

In optical fiber communications the attenuation is usually expressed in decibels

be intrinsic (caused by the interac...
of the glass) or extrinsic (caused by impurities within the glass).

3.3.1 Intrinsic absorption

An absolutely pure silicate glass has little intrinsic absorption due to its basic material structure in the near-infrared region. However, it does have two major intrinsic absorption mechanisms at optical wavelengths which leave a low intrinsic absorption window over the 0.8 to 1.7 μm wavelength range, as illustrated in Figure 3.1, which shows a possible optical attenuation against wavelength characteristic for absolutely pure glass [Ref. 3]. It may be observed that there is a fundamental absorption edge, the peaks of which are centred in the ultraviolet wavelength region. This is due to the stimulation of electron transitions within the glass by higher energy excitations. The tail of this peak may extend into the window region at the shorter wavelengths, as illustrated in Figure 3.1. Also in the infrared